

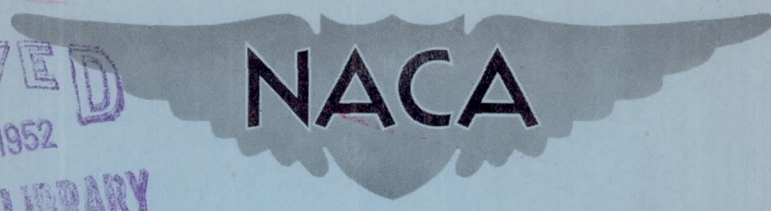
CONFIDENTIAL

Copy 217
RM L52J08

RM-L 52J-08

NACA RM L52J08

RECEIVED
NOV 25 1952
TECHNICAL LIBRARY



RESEARCH MEMORANDUM

INVESTIGATION AT HIGH SUBSONIC SPEEDS OF BODIES MOUNTED
FROM THE WING OF AN UNSWEPT-WING—FUSELAGE MODEL,
INCLUDING MEASUREMENTS OF BODY LOADS

By H. Norman Silvers and Thomas J. King, Jr.

CANCELLED
Classification
CHANGED TO *Uncl.*
NACA Res. Abstract 114-57
J. Leader

Langley Aeronautical Laboratory
Langley Field, Va.

TECHNICAL LIBRARY
AIRCRAFT MANUFACTURING CO.
951-951 SEPULVEDA BLVD.
LOS ANGELES 45, CALIF.
CALIFORNIA

CLASSIFIED DOCUMENT

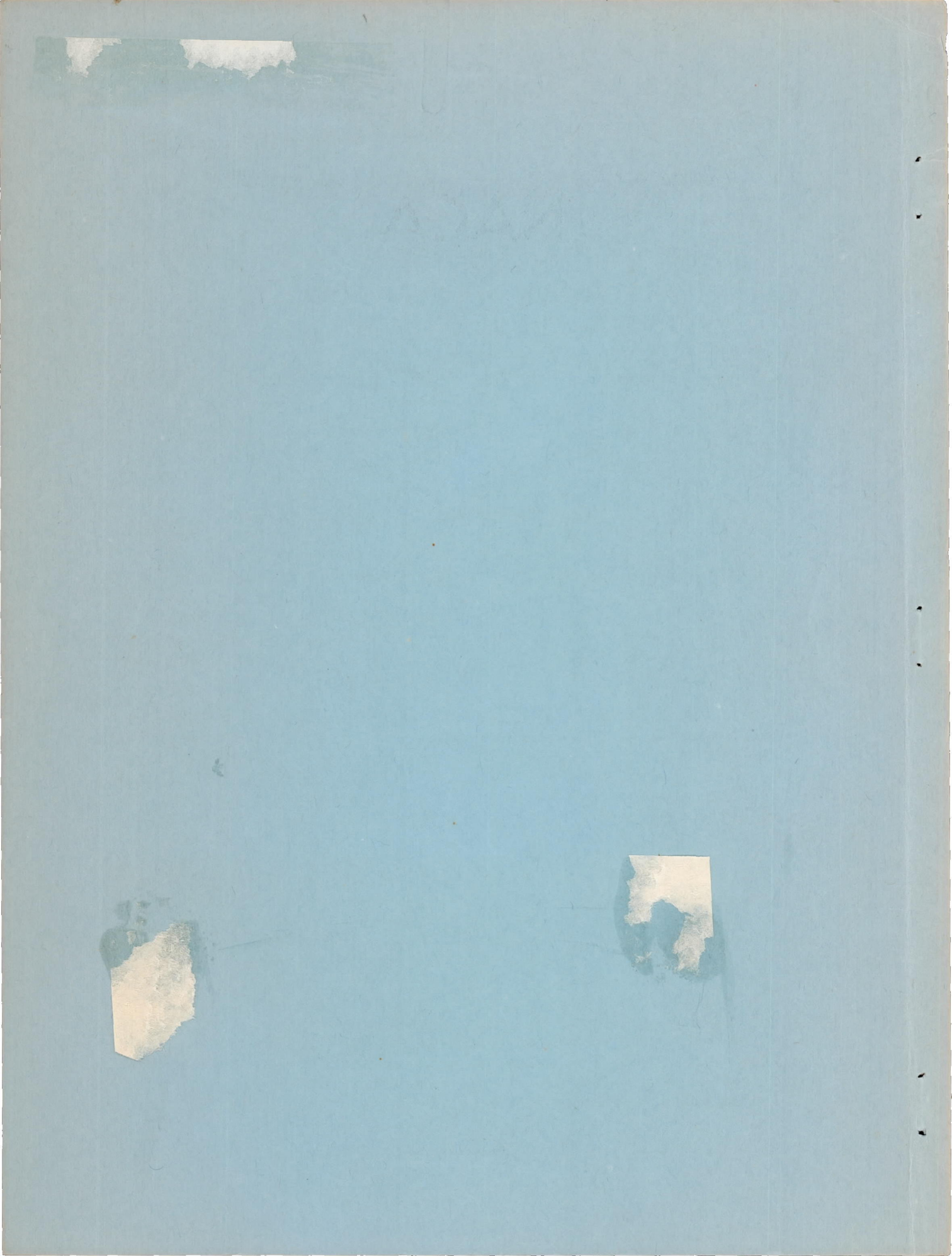
This material contains information affecting the National Defense of the United States within the meaning of the espionage laws, Title 18, U.S.C., Secs. 793 and 794, the transmission or revelation of which in any manner to unauthorized person is prohibited by law.

NATIONAL ADVISORY COMMITTEE FOR AERONAUTICS

WASHINGTON

November 14, 1952

CONFIDENTIAL



NATIONAL ADVISORY COMMITTEE FOR AERONAUTICS

RESEARCH MEMORANDUM

INVESTIGATION AT HIGH SUBSONIC SPEEDS OF BODIES MOUNTED
FROM THE WING OF AN UNSWEPT-WING—FUSELAGE MODEL,
INCLUDING MEASUREMENTS OF BODY LOADS

By H. Norman Silvers and Thomas J. King, Jr.

SUMMARY

An investigation has been made with the dual purpose of determining the effect of two bodies in various positions, symmetrically located from the plane of symmetry, on the aerodynamic characteristics of a wing-fuselage model and of determining the aerodynamic loads on one of the two bodies. The wing of the model had a straight 0.5-chord line, was of aspect ratio 4, taper ratio 0.6, and had NACA 65A006 airfoil sections. The bodies were investigated with two pylon lengths at 0.33 semispan, for one pylon length at 0.96 semispan, and mounted directly to the wing tip so that the body center line was in the chord plane of the wing and located at 1.04 semispan.

The results indicate that some of the most significant effects of the bodies on the aerodynamic characteristics of the model were obtained for the direct-mounted tip bodies which gave a large increase in the lift-curve slope of the basic model and the lowest drag of any installation investigated. Of the bodies investigated at 0.33 semispan, lower installation drag coefficients were obtained with the bodies on the short pylons than on the long pylons.

The force and moment coefficients of the bodies in the presence of the wing-fuselage and pylons indicate that Mach number has less effect on the character of the curves than changes in model angle of attack which produced abrupt and significant changes in the body aerodynamic characteristics. In general, similar characteristics were shown for both positions of the bodies at 0.33 semispan and also for both positions of the bodies at the wing tip. At the wing tip the bodies were more unstable in pitch and showed a greater effect of angle of attack on yawing moment and side force than was obtained in inboard positions. The static force and moment data of the bodies in the presence of the model indicated that upon release at an angle of attack of 4° from an inboard location the bodies would initially tend to pitch only slightly

and would tend to nose out in yaw while moving toward the wing tip. Release of tip-mounted bodies however would seem to involve some hazard of collision of body and airplane since the body forces and moments, in addition to being more substantial, would initially tend to make the bodies pitch up and nose in. The lift carried by the direct-mounted tip body appeared sufficient to support considerable body weight.

INTRODUCTION

The National Advisory Committee for Aeronautics is conducting investigations of nacelles and external stores for use on high-speed aircraft. These investigations are concerned with an evaluation of the effects of body positioning with respect to the wings and of changes in body shape. Considerable information has been accumulated in the transonic speed range on the effects of positioning of bodies mounted directly to wings without pylon members (refs. 1 to 4). A comprehensive investigation also has been made of changes in the geometric parameters of a pylon-suspended body at subsonic speeds (ref. 5). The information in the foregoing papers should provide useful design data for those concerned with the effects of bodies on the over-all performance of airplanes. It has however little general application to some specialized phases of external store and nacelle design; namely, body-loading conditions. Apart from the desirability of obtaining this information for structural design of the installations, it is of considerable current interest for application to the release of external stores at high speed and to missile launching. The program has been extended to provide this information, and the results presented in this paper are a part of this program. In the present paper are shown the changes in body force and moment characteristics at high subsonic speeds for several locations of bodies and pylons on an unswept wing of aspect ratio 4.0.

The results presented herein were obtained generally at Mach numbers from 0.50 to 0.91 over an angle-of-attack range which was dependent upon the body loads because of limiting load factors of the strain-gage-balance measuring system. Four positions of two bodies symmetrically located from the plane of symmetry were investigated; two vertical locations of a pylon-suspended body located at 0.33 semispan, a pylon-suspended body below the wing tip at 0.96 semispan, and a body mounted at 1.04 semispan and in the chord plane of the wing. The length of the longer pylon of the inboard installation was established as a near-optimum vertical location of the body for minimum installation drag (ref. 5), while the shorter lengths of pylon for both the inboard and tip installations are those thought to give a practical vertical location for proper ground clearance when used on low-slung jet aircraft. No stabilizing fins were added to the bodies of this investigation.

SYMBOLS

C_L	lift coefficient, $Lift/qS_W$
C_D	drag coefficient, $Drag/qS_W$
C_{D_n}	installation-drag coefficient, $(C_{D_{model}} + bodies - C_{D_{model}}) \frac{S_W}{2S_b}$
C_m	pitching-moment coefficient referred to $0.25\bar{c}$ of wing, Pitching moment/ $qS_W\bar{c}$
$C_{L_{b_l}}$	body lift coefficient, $Body\ lift/qS_b$
$C_{D_{b_l}}$	body drag coefficient, $Body\ drag/qS_b$
$C_{m_{b_l}}$	body pitching-moment coefficient referred to $0.462l_b$, Body pitching moment/ $qS_b l_b$
$C_{n_{b_l}}$	body yawing-moment coefficient referred to $0.462l_b$, Body yawing moment/ $qS_b l_b$
$C_{l_{b_l}}$	body rolling-moment coefficient referred to the body center line, $Body\ rolling\ moment/qS_b l_b$
$C_{Y_{b_l}}$	body side-force coefficient, $Body\ side\ force/qS_b$
q	free-stream dynamic pressure
S_W	wing area, 2.25 sq ft
S_b	maximum frontal area of body, 0.0215 sq ft
\bar{c}	mean aerodynamic chord of wing, 0.765 ft, $\frac{2}{S_W} \int_0^{b/2} c^2 dy \quad (\text{using theoretical tip})$
c	local wing chord, ft
b	wing span, 3.0 ft

l_b	body length, 1.544 ft
l_f	fuselage length, 4.10 ft
d_b	body diameter, ft
d_f	fuselage diameter, ft
V	free-stream air velocity, fps
a	free-stream velocity of sound, fps
M	Mach number, V/a
ρ	mass density of air, slugs/cu ft
α	complete-model angle of attack, deg
θ_b	angle of the body center line with respect to the wing chord line, deg
ϕ_b	angle of the body center line with respect to the plane of symmetry, deg

$$C_{L\alpha} = \left(\frac{\partial C_L}{\partial \alpha} \right)_M$$

$$C_{mC_L} = \left(\frac{\partial C_m}{\partial C_L} \right)_M$$

APPARATUS AND MODEL

A drawing showing the model with the various positions of bodies tested is presented in figure 1. The wing was constructed of aluminum and had NACA 65A006 airfoil sections parallel to the free stream. The fuselage also was constructed of aluminum and was formed by parabolic-arc sections, ordinates for which are given in table I.

The model was attached to the supporting sting by an internal strain-gage balance. The forces and moments of the model with and without the two bodies were measured by the balance and recorded automatically. Photographs of the model mounted in the tunnel, showing the bodies in the inboard position, are shown in figure 2.

The body was generated by revolution of a profile made up of ogival nose and tail sections, between which was a parallel-sided section. The fineness ratio of the body was 9.34. Ordinates of the body are presented in table II. Two general installations of bodies were used - one was a pylon installation which used two lengths of pylon at $0.33\frac{b}{2}$ and one length of pylon at $0.96\frac{b}{2}$, and the other was a direct-mounted wing-tip installation having the center line of the body in the chord plane of the wing at $1.04\frac{b}{2}$. The bodies were located in all positions so that the distances from the noses of the bodies to the 0.5-chord line, which was straight on this wing, were constant.

For each configuration a body was tested on each wing semispan. The body instrumented with the six-component strain-gage balance was mounted from the left wing, while a solid wooden body was attached to the right wing. The body housing the balance was constructed of plastic impregnated with fiber glass. A cutaway drawing showing the installation of the balance with the clearance gaps between the pylon or wing tip and the body is presented in figure 3.

The pylons were unswept and had NACA 64A010 airfoil sections parallel to the free stream.

The origin of the axis of the body balance remained fixed with respect to the body length for all positions of the body. The pitching-moment-axis location relative to the local chord changed slightly for each body position because of the wing taper. Tabulated below are the locations of the pitching-moment axis for each body position based on both the local wing chord and the body length:

Configuration	Spanwise location, wing semispans	Pitching-moment axis, percent local c	Pitching-moment axis, percent body length
Inboard	0.33	45.6	46.2
Underwing tip	.96	44.1	46.2
Tip	1.04	43.6	46.2

The alinement of the bodies in the pitch plane and of the bodies and pylons in the yaw plane was checked and found to be within 0.10° of the design angular positions. Because centering pins were employed on all components of each configuration, the repeatability of angular alinement values was good.

TESTS AND RESULTS

The tests were conducted in the Langley high-speed 7- by 10-foot tunnel through a Mach number range that usually extended from 0.50 to 0.91. The angle-of-attack range investigated was restricted by the load limits of the body balance and therefore varied for each position of the body. A model yaw angle of zero was maintained for all tests of this investigation.

The results obtained on the complete model are presented as the lift, drag, and pitching-moment coefficients of the model without and with the two bodies in the several locations on the wing of the model. Forces and moments of the complete model are presented with respect to the wind axes, with the pitching moment being presented about the 0.25-chord point of the mean aerodynamic chord.

The characteristics of the bodies in the presence of the model are presented as six-component force and moment measurements varying with model angle of attack. For clarity of comparisons of these data with the increments taken from complete-model data, lift and drag forces have been presented about the wind axes as shown in figure 4. Other body force and moment results are presented relative to the body axes. The body coefficients are based upon the maximum frontal area of the body and, in the case of moments, also upon the body length.

The body coefficients are the forces and moments of the body in the presence of the wing, fuselage, and pylons, and hence include the interference of these parts on the body as well as the forces and moments of the body alone. The direct-mounted tip body, having no pylon, does not experience pylon interference. Also presented in this paper are the incremental effects of the bodies on the drag characteristics of the model obtained from the total drag data of the model with and without bodies. This increment is defined as the installation-drag coefficient C_{Dn} and was obtained by the following equation

$$C_{Dn} = \left(C_{D_{\text{model} + \text{bodies}}} - C_{D_{\text{model}}} \right) \frac{S_w}{2S_b}$$

The installation-drag coefficient C_{Dn} then includes, for the installations using pylons, the drag of the pylons plus interference as well as the drag of the bodies plus interference. Thus a direct comparison of the body drag coefficient with the incremental drag coefficient would yield pylon drag plus pylon interference drag plus the interference drag due to the bodies on the wing and fuselage.

Lift-curve and pitching-moment-curve slopes of the model with and without the bodies were taken at zero lift coefficient. The body pitching-moment-curve slopes were taken at zero angle of attack. Because of several nonlinearities, no body lift-curve slopes are presented.

The Reynolds number based on the mean aerodynamic chord is presented in figure 5 as a function of Mach number.

CORRECTIONS

Blocking corrections applied to Mach number and dynamic pressure were determined by the velocity-ratio method of reference 6, which utilizes experimental pressures measured at the tunnel wall opposite the model. Over the Mach number range investigated good agreement was obtained between these corrections and those obtained theoretically (ref. 7). The correction to Mach number increased slightly with increase in speed and at $M = 0.90$ was 0.01.

The jet-boundary corrections applied to lift and drag were calculated by the method of reference 8. The corrections to pitching moment were considered negligible. No support tares have been applied, but as indicated in reference 9 they are believed to be small. Drag data have been corrected to correspond to a pressure at the base of the fuselage equal to free-stream static pressure. Base pressure was determined by measuring the pressure at a point inside the fuselage about 9 inches forward of the base. This correction, which was added to the measured drag coefficient, amounted to a drag-coefficient increment that increased from a value of 0.0010 at $M = 0.50$ to 0.0030 at $M = 0.91$. It was found during this investigation that the bodies had no effect on the fuselage base pressure.

Corrections have been applied to the angle of attack of the model due to deflection of the support system under load. No correction has, however, been applied to the results presented in this paper to account for aeroelastic distortion of the wing since these corrections are small (ref. 10) for the model without bodies.

No correction has been made to the body angles of attack or yaw due to the deflection of the body balance under load. A deflection calibration has however been made and the results presented in moment-coefficient form are shown in figure 6 for Mach numbers giving maximum and minimum dynamic pressures. These results indicate that the body deflection due to a body pitching load is usually less than 0.15° and due to a yawing load less than 0.25° .

DISCUSSION

Complete Model

The basic data obtained for the model without bodies are presented in figure 7, while the data obtained with the bodies in several locations on the model are presented in figure 8. The effects of the bodies in several locations on the aerodynamic characteristics of the model are summarized in figure 9.

The results show that the bodies generally produce a stabilizing influence on the model as indicated by $C_{m_{C_L}}$ (fig. 9). As will be shown later in the body loading results, the bodies in both the inboard and tip positions show unstable pitching-moment characteristics. The stabilizing effect of the bodies on the complete model therefore can be due in part to the body lift and its location rearward of the moment center of the complete model. Other factors are the body drag and its location below the moment center of the complete model, as well as the interference effects of the bodies and pylons on the wing loading characteristics.

The degree of stability contributed by the bodies is dependent upon the body location. The bodies in the inboard location on short pylons are seen to produce little change in the stability of the model, while the bodies on the longer pylons provide a stabilizing effect on the model. The stabilizing effect of the installation is increased as the bodies are moved outboard - resulting in the maximum increase in stability being produced by the direct-mounted tip bodies (the pylon-suspended tip bodies are designated herein as the underwing tip configuration). The largest increase in stability below the Mach number for pitching-moment break occurs at a Mach number of about 0.85 for the direct-mounted tip bodies and is equivalent to about a 3.5-percent change in the aerodynamic-center location based on the mean aerodynamic chord.

An inboard mounting of the bodies is seen to reduce the lift-curve slope of the model a small amount up to a Mach number of 0.77 where some increase occurs up to a little past the initial lift-curve-slope break. Of primary interest, however, is the substantial increase in $C_{L_{\alpha}}$ produced by the tip locations of the bodies. An increase in $C_{L_{\alpha}}$ may be expected with tip mountings of the bodies because of the end-plate action of the bodies, but the increases that were obtained in this investigation (using an unswept wing) are substantially larger than those found for sweptback wings (unpublished data). For a semispan wing sweptback 45° with aspect ratio 6 a direct-mounted tip body has

given an increase in $C_{L\alpha}$ of the model of the order of 12 percent. The largest increase in $C_{L\alpha}$ due to the direct-mounted tip bodies of the present investigation is about 28 percent. Somewhat smaller, although still appreciable, increases are seen to be obtained with the underwing tip bodies.

The lowest increment in drag due to the bodies is found for the direct-mounted tip bodies (fig. 9). Some reduction in installation drag can be expected with this mounting of the bodies because this installation does not use a drag-producing pylon member. It appears that the end-plating of the bodies by increasing the effective aspect ratio of the wing and thus reducing the drag-due-to-lift may further reduce the installation drag. This latter effect would of course be dependent upon lift coefficient whereas the former effect may be largely independent of lift coefficient. It is seen from the data (fig. 9) that at the lower lift coefficients the increments in drag due to the direct-mounted tip bodies are only slightly less than those shown for other mountings of the bodies. As the lift is increased, however, large reductions in the increment in drag of the direct-mounted tip installations occur compared to the drag of the other installations. In fact, at a lift coefficient of 0.4 the drag of the model with direct-mounted tip bodies is seen to be less than that of the model without bodies. For a better conception of the increments in drag due to the body installation, figure 10 is presented and shows the increments in drag due to installations based on the maximum frontal area of the body (defined by the symbol C_{Dn}).

It is of interest to note that, although the longer pylon of the inboard-located bodies was selected for minimum installation drag from results presented in reference 5, which were obtained on a model with a 45° sweptback wing, it gave higher drag than the installation with the shorter pylons and the drag was, in fact, the highest of all configurations tested on the straight-wing model of this investigation. The contradictory nature of these results may be due to the difference in sweep angles of the wings used in the two investigations. Another factor that may contribute to this condition is the shape of the body. In reference 5 the body shape was generated by revolution of an airfoil section, while in this investigation the body employed a constant-diameter section for the body midportion. Such differences can alter interference characteristics, and thus the apparent optimum pylon length.

Bodies in the Presence of the Model

In interpreting the body forces and moments it should be kept in mind that the measurements were made with the instrumented body on the

left wing of the model. It is also well to remember that the lines of action of the forces and moments are as indicated in figure 4. The coefficients of forces and moments of the bodies in several locations on the wing are presented in figure 11 as a function of model angle of attack. These data indicate that, in general, similar aerodynamic characteristics are shown for both vertical locations of the inboard-mounted bodies and also for both positions of the tip bodies, but some important differences exist between the characteristics of inboard-mounted and tip-mounted configurations. Change in Mach number has less effect upon the character of the curves than change in model angle of attack which produces some abrupt and apparently significant changes in some of the coefficients.

Although the bodies in the inboard position carry positive lift, they have a negative lift-curve slope at the lower angles of attack and Mach numbers. At Mach numbers greater than about 0.80 the lift-curve slopes change from negative to positive. The direct-mounted tip body has a large and near-linear positive increase in lift coefficient with increase in angle of attack. The body lift coefficients obtained at the higher angles of attack appear sufficiently large to support considerable body weight. The underwing tip body, although having somewhat smaller positive lift-curve slopes at angles of attack near zero, shows an abrupt break to a negative slope in the lift curve at angles of attack of the order of 1° to 2° . In the inboard location the bodies are unstable in pitch for both lengths of pylon, and the outboard bodies show greater pitch instability than the inboard bodies with the greatest instability being shown for the direct-mounted tip body.

In order to provide a quantitative expression of the stability characteristics of the instrumented body, figure 12 has been prepared and presents the slope of the body pitching-moment coefficients with angle of attack as a function of Mach number.

The slope of the pitching moment of the isolated body has been calculated by the method of reference 11 and is represented in figure 12 by the symbol point.

It is seen from these data that, compared to the calculated stability of the isolated body, interference effects of the model and pylon on the body are stabilizing for the pylon-suspended bodies, and particularly for the inboard location of the bodies. For the direct-mounted tip bodies interference appears to be destabilizing.

The drag coefficients of the inboard-mounted bodies show a near-linear increase with increase in angle of attack at the higher Mach numbers, while a sharp trough develops in the drag curves at low angles of attack for the tip-mounted bodies. As expected from the installation symmetry, the curve of the direct-mounted tip body is symmetrical about zero angle of attack.

The lateral components show that for the inboard bodies negative slopes in both yawing-moment and side-force coefficients result from increases in model angle of attack in a fairly linear manner with the rolling moment having a small negative value and showing little change with angle of attack. Both tip-mounted body installations are seen to develop severe breaks in both the yawing-moment and rolling-moment curves and in the side-force curves for the direct-mounted tip body. The yawing-moment breaks resemble the troughs of the drag curves with the yawing-moment trough of the direct-mounted tip body being centered about zero angle of attack. The trough of the yawing-moment curve of the underwing tip body moves through zero angle of attack from an initial positive α with increase in Mach number. The tip-mounted bodies are seen to carry large negative values of side force for most positive angles of attack, and these values increase almost linearly with model angle of attack.

Body force and moment coefficients are of interest in providing some indication of the initial path that a body might take upon release. In the following discussion the estimated release characteristics of the configurations tested are briefly summarized. For simplicity it is assumed that release would take place at an angle of attack of 4° . It should be understood that different release characteristics may exist at other angles of attack. It would appear that the bodies if released from the inboard location at $\alpha = 4^\circ$ would initially tend to pitch very little, but would nose out in yaw while moving toward the wing tip. Rolling moment does not seem to be of critical importance in this location. The only effect of increasing the speed to Mach numbers of the order of $M = 0.86$ for inboard bodies appears to be that some nose-down pitching motion would be introduced. Release of the underwing tip bodies would appear to result in initial pitching up and a yawing out at low speeds, yawing in at high speeds, and moving outboard at all speeds due to large body side forces. Release of the direct-mounted tip bodies would seem to involve the greatest hazard, since the bodies would initially tend to pitch up and nose in. These conditions, being produced by substantial pitching and yawing moments and combined with the rather large positive lift carried by the direct-mounted tip bodies, X suggest the possibility of body-airplane collision after release.

CONCLUSIONS

An investigation at high subsonic speeds of two bodies mounted from the wing of an unswept-wing—fuselage model, including the measurements of body loads, indicates the following conclusions:

1. Some of the most significant effects of the bodies on the aerodynamic characteristics of the model were found for the direct-mounted

tip bodies which gave a large increase in lift-curve slope of the model and the lowest installation drag of all configurations investigated.

2. Of the inboard-located bodies, somewhat lower installation-drag coefficients were obtained with the short pylons than with long pylons.

* 3. The force and moment coefficients of the bodies in the presence of the wing-fuselage and pylon indicate that a change in Mach number has less effect on the character of the curves than changes in model angle of attack which produced abrupt and significant changes in the body aerodynamic characteristics.

4. In general, similar body characteristics were shown for both positions of the bodies at 0.33 semispan and also for both positions of the bodies at the wing tip. At the wing tip the bodies were more unstable in pitch and showed a greater effect of angle of attack on yawing moment and side force than at the inboard locations.

5. It would appear from the static forces and moments on the bodies at 4° angle of attack that upon release from the inboard location the bodies would initially tend to pitch only slightly but would tend to nose out in yaw while moving toward the wing tip. Release of tip-mounted bodies would seem to involve some hazard of body-airplane collision since the body forces and moments, in addition to being substantial, would initially tend to make the bodies pitch up and nose in. The lift carried by the direct-mounted tip bodies appeared sufficient to support considerable body weight. Tip-mounted bodies also carried large side-force coefficients which would initially tend to result in outboard movement of the bodies upon release.

Langley Aeronautical Laboratory,
National Advisory Committee for Aeronautics,
Langley Field, Va.

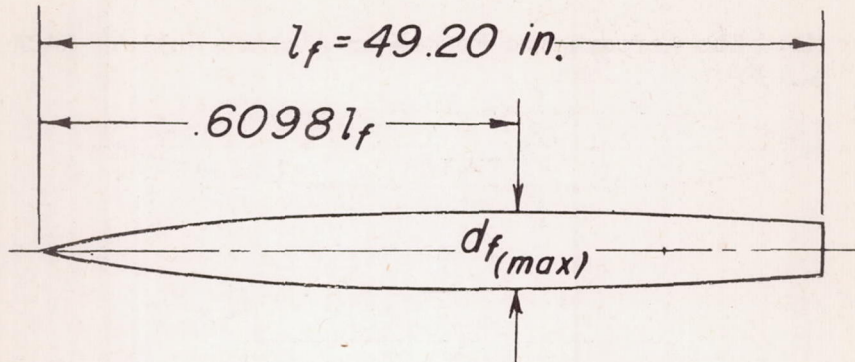
REFERENCES

1. Pepper, William B., Jr., and Hoffman, Sherwood: Transonic Flight Tests To Compare the Zero-Lift Drag of Underslung and Symmetrical Nacelles Varied Chordwise at 40 Percent Semispan of a 45° Sweptback, Tapered Wing. NACA RM L50G17a, 1950.
2. Hoffman, Sherwood: Comparison of Zero-Lift Drag Determined by Flight Tests at Transonic Speeds of Pylon, Underslung, and Symmetrically Mounted Nacelles at 40 Percent Semispan of a 45° Sweptback Wing and Body Combination. NACA RM L51D26, 1951.
3. Silvers, H. Norman, King, Thomas J., Jr., and Pasteur, Thomas B., Jr.: Investigation of the Effects of a Nacelle at Various Chordwise and Vertical Positions on the Aerodynamic Characteristics at High Subsonic Speeds of a 45° Sweptback Wing With and Without a Fuselage. NACA RM L51H16, 1951.
4. Hoffman, Sherwood, and Pepper, William B., Jr.: Transonic Flight Tests To Determine Zero-Lift Drag and Pressure Recovery of Nacelles Located at the Wing Tips on a 45° Sweptback Wing and Body Combination. NACA RM L51K02, 1952.
5. Spreemann, Kenneth P., and Alford, William J., Jr.: Investigation of the Effects of Geometric Changes in an Underwing Pylon-Suspended External-Store Installation on the Aerodynamic Characteristics of a 45° Sweptback Wing at High Subsonic Speeds. NACA RM L50L12, 1951.
6. Hensel, Rudolf W.: Rectangular-Wind-Tunnel Blocking Corrections Using the Velocity-Ratio Method. NACA TN 2372, 1951.
7. Herriot, John G.: Blockage Corrections for Three-Dimensional-Flow Closed-Throat Wind Tunnels, With Consideration of the Effect of Compressibility. NACA Rep. 995, 1950. (Supersedes NACA RM A7B28.)
8. Gillis, Clarence L., Polhamus, Edward C., and Gray, Joseph L., Jr.: Charts for Determining Jet-Boundary Corrections for Complete Models in 7- by 10-Foot Closed Rectangular Wind Tunnels. NACA ARR L5G31, 1945.
9. Osborne, Robert S.: High-Speed Wind-Tunnel Investigation of the Longitudinal Stability and Control Characteristics of a $\frac{1}{16}$ -Scale Model of the D-558-2 Research Airplane at High Subsonic Mach Numbers and at a Mach Number of 1.2. NACA RM L9C04, 1949.

10. Wiggins, James W., and Kuhn, Richard E.: Wind-Tunnel Investigation of the Aerodynamic Characteristics in Pitch of Wing-Fuselage Combinations at High-Subsonic Speeds. Sweep Series. NACA RM L52D18, 1952.
11. Munk, Max M.: The Aerodynamic Forces on Airship Hulls. NACA Rep. 184, 1924.

TABLE I.- FUSELAGE ORDINATES

[Basic fineness ratio 12, actual fineness ratio 9.8 achieved by cutting off rear portion of body]



Ordinates, percent length	
Station	Radius
0	0
.61	.28
.91	.36
1.52	.52
3.05	.88
6.10	1.47
9.15	1.97
12.20	2.40
18.29	3.16
24.39	3.77
30.49	4.23
36.59	4.56
42.68	4.80
48.78	4.95
54.88	5.05
60.98	5.08
67.07	5.04
73.17	4.91
79.27	4.69
85.37	4.34
91.46	3.81
100.00	3.35

L. E. radius = .00061

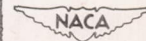
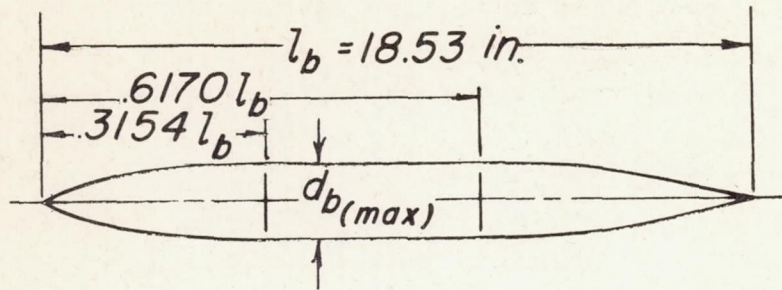


TABLE II.- BODY ORDINATES

[Fineness ratio 9.34]



Ordinates, percent length	
Station	Radius
0	0
.36	.30
1.21	.73
3.04	1.44
4.87	2.09
6.71	2.65
8.26	3.07
9.15	3.29
9.69	3.44
10.84	3.70
11.99	3.94
13.14	4.12
14.29	4.30
15.44	4.44
17.74	4.70
20.04	4.92
22.34	5.08
24.64	5.20
26.94	5.30
29.24	5.34
31.54	5.36
61.70	5.36
68.69	5.20
74.95	4.76
81.22	3.94
87.48	2.76
90.60	2.11
93.75	1.42
96.89	.72
98.44	.36
100.00	0

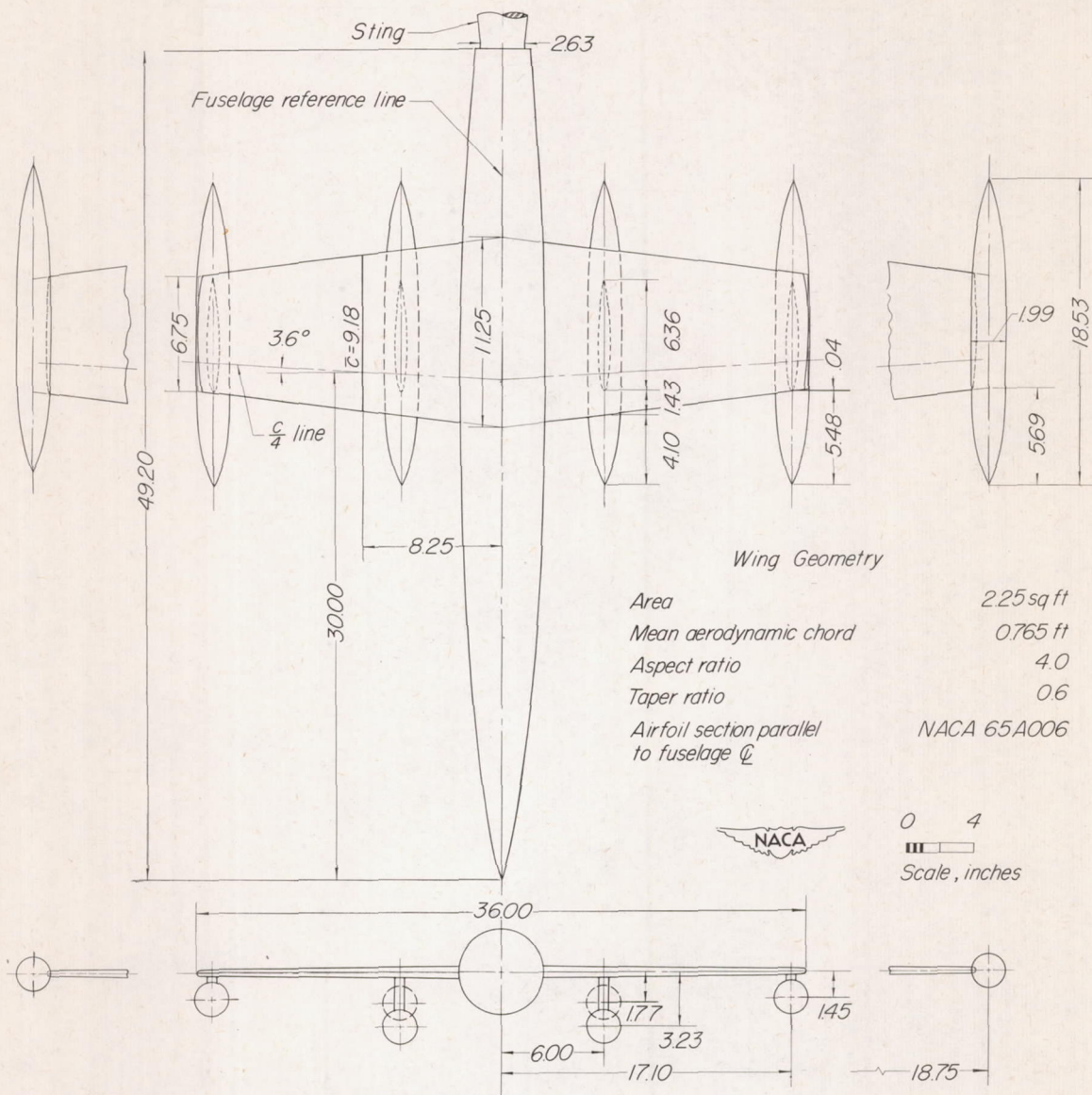


Figure 1.- Model of wing, fuselage, and bodies showing various locations of the bodies as tested on the sting support system in the Langley high-speed 7- by 10-foot tunnel.

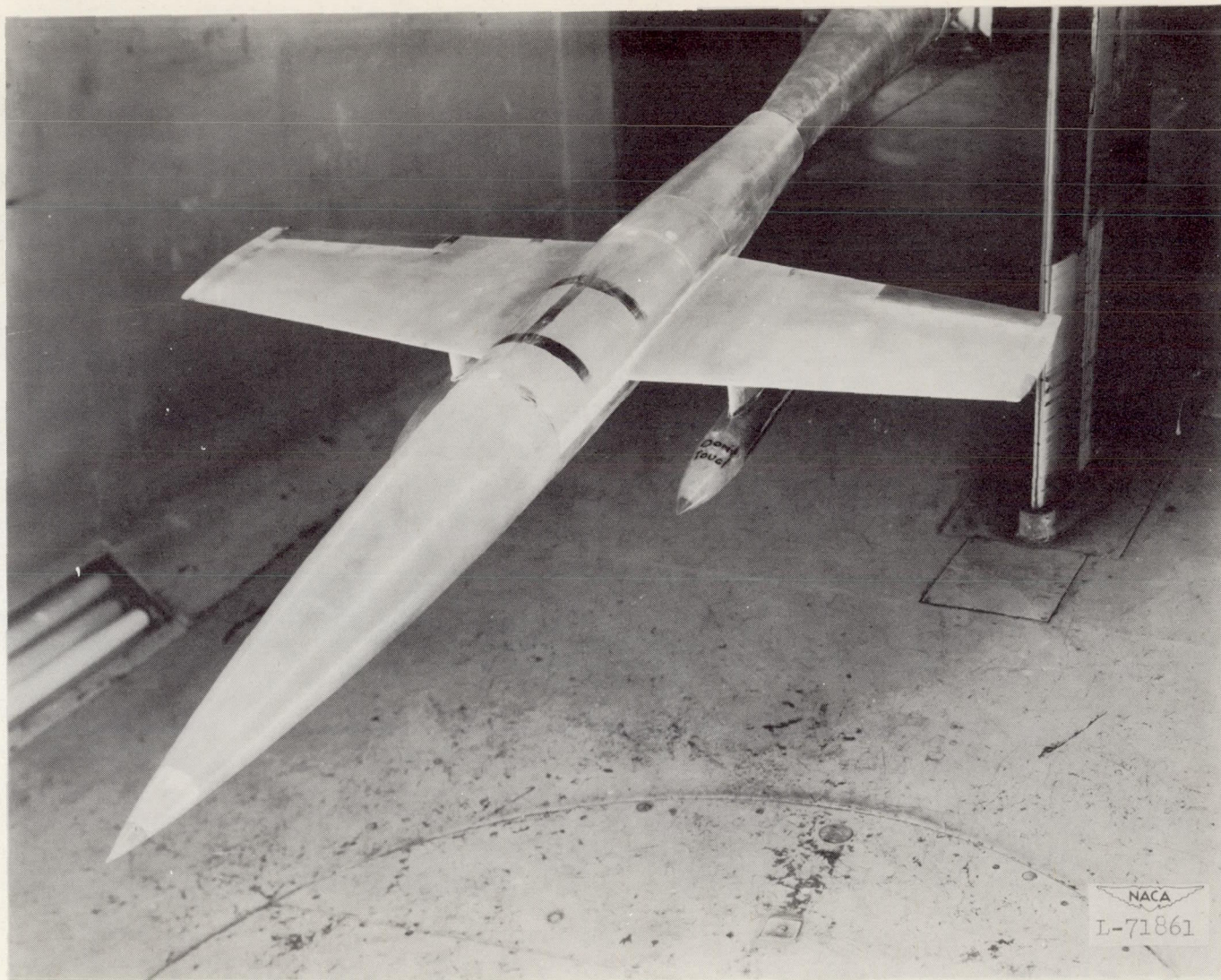


Figure 2.- Model with bodies mounted in inboard position and on long pylons.

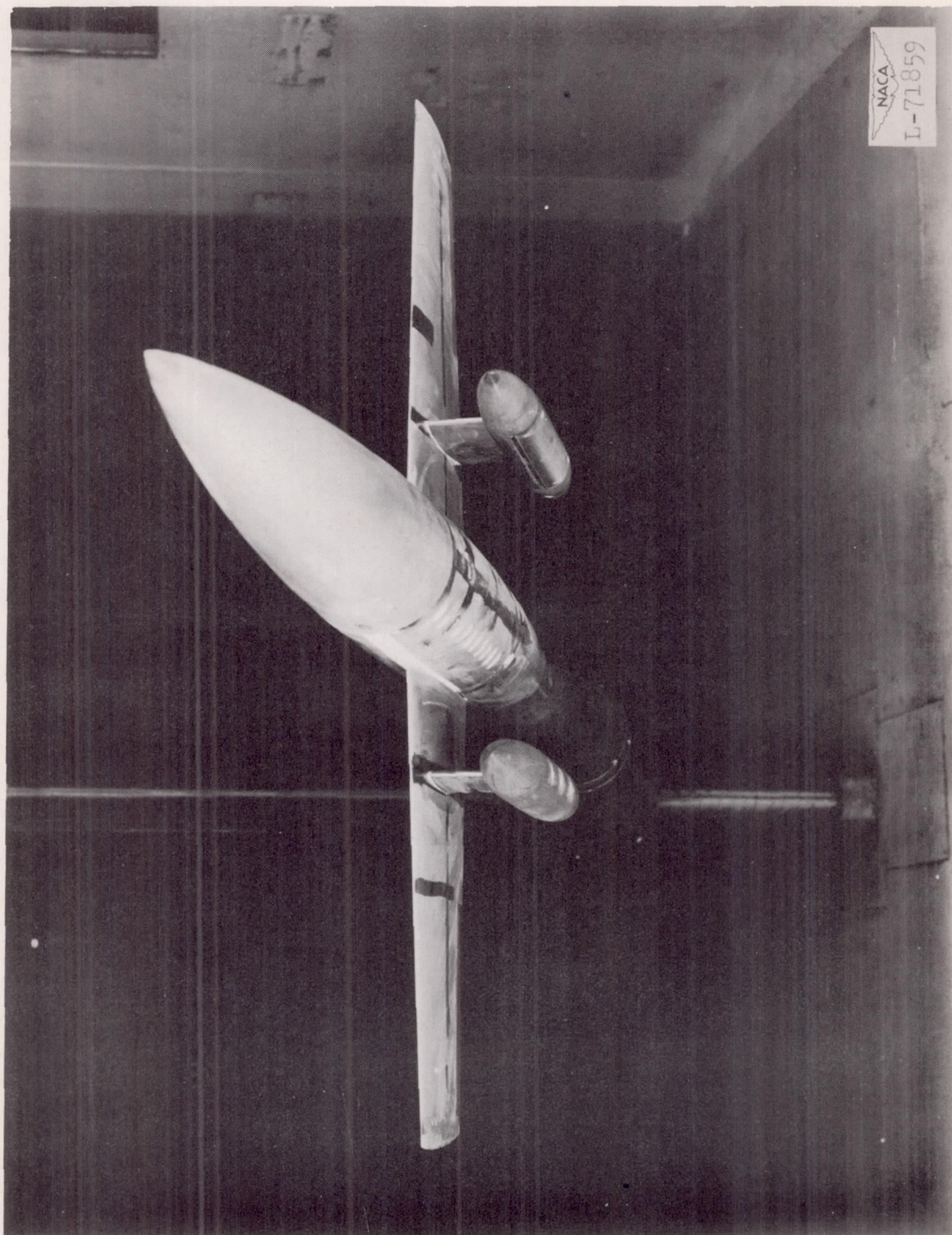


Figure 2. - Concluded.

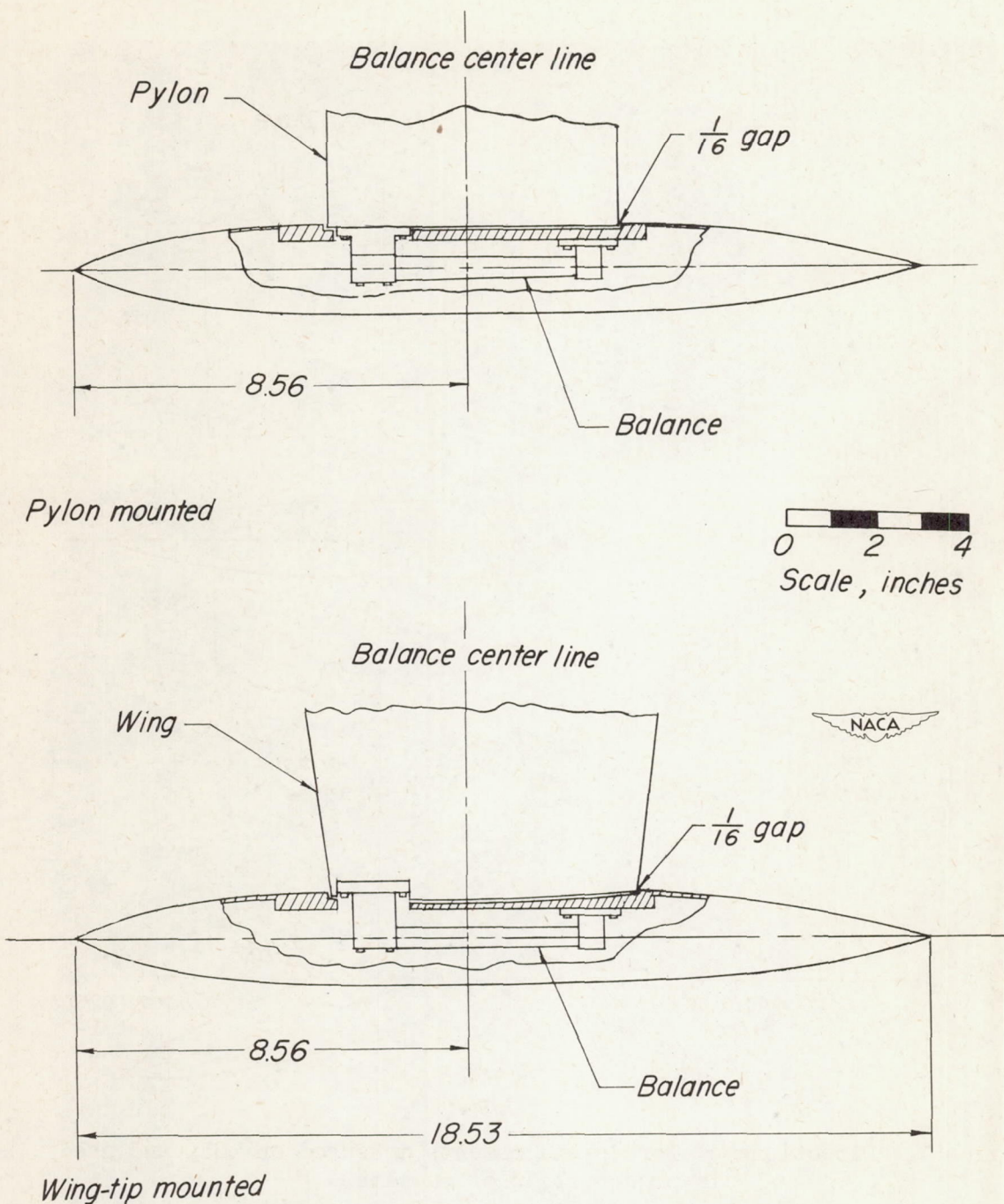


Figure 3.- Cutaway drawing showing instrumented body as mounted on pylons and wing tip.

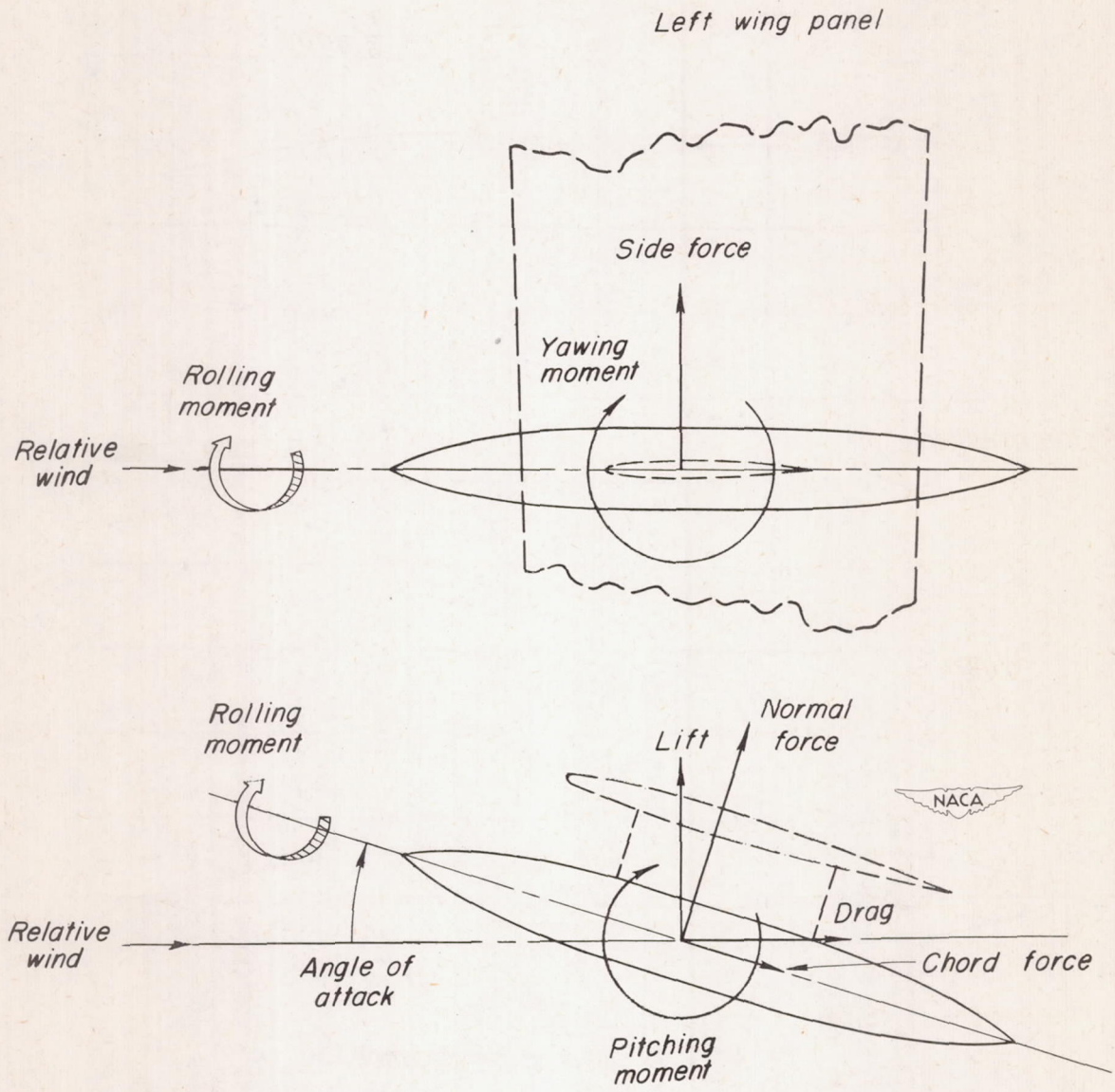


Figure 4.- Directions of forces and moments measured on body and used in presentation of results.

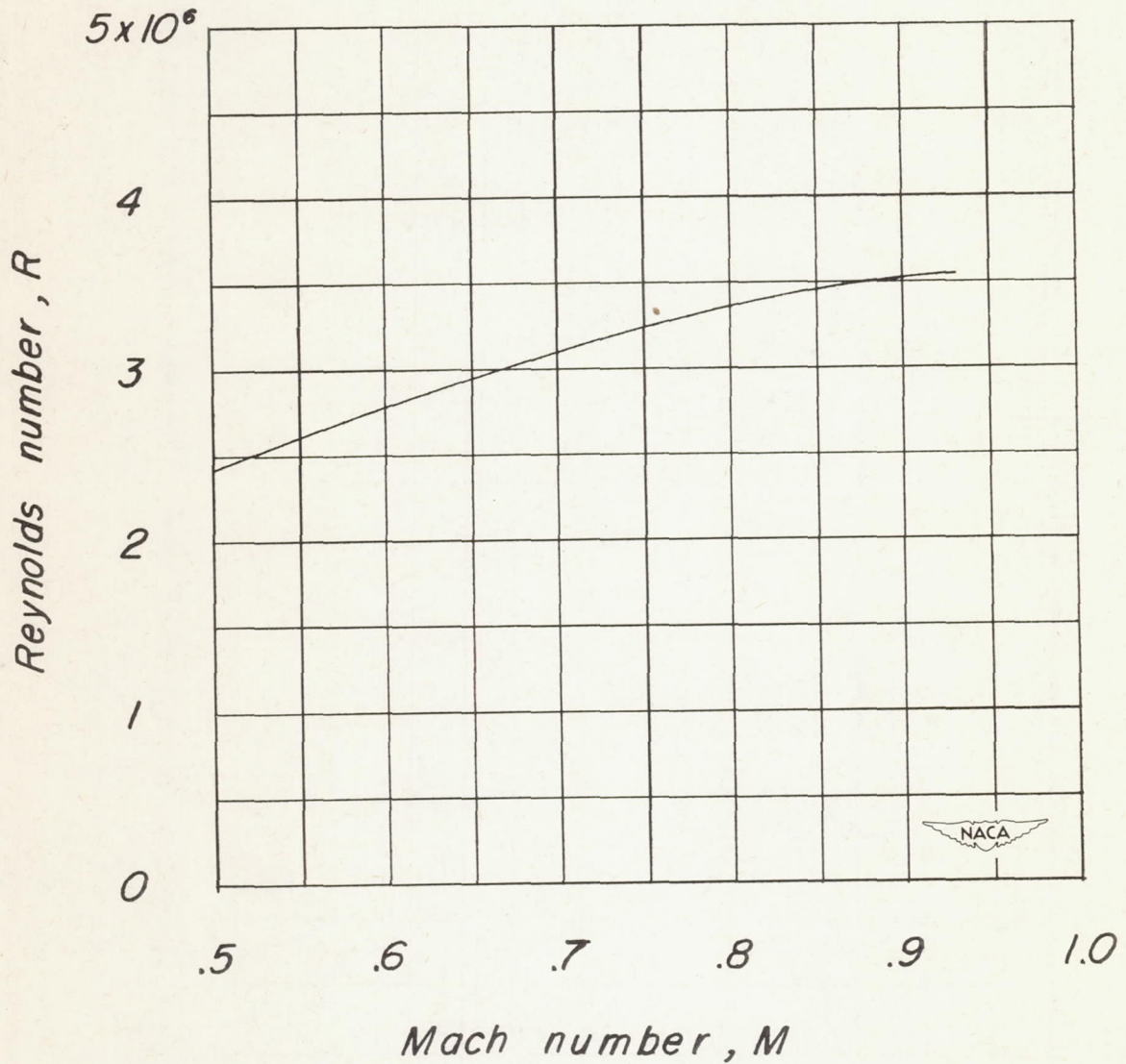


Figure 5.- Variation of Reynolds number with Mach number for model.

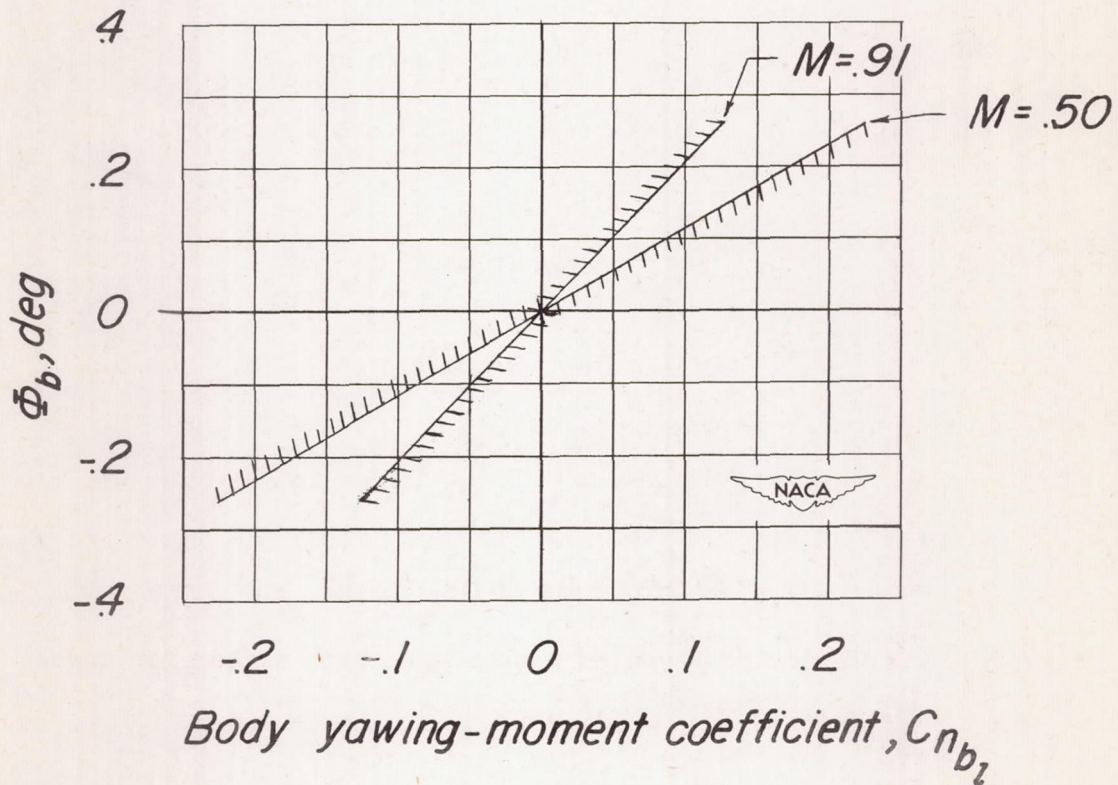
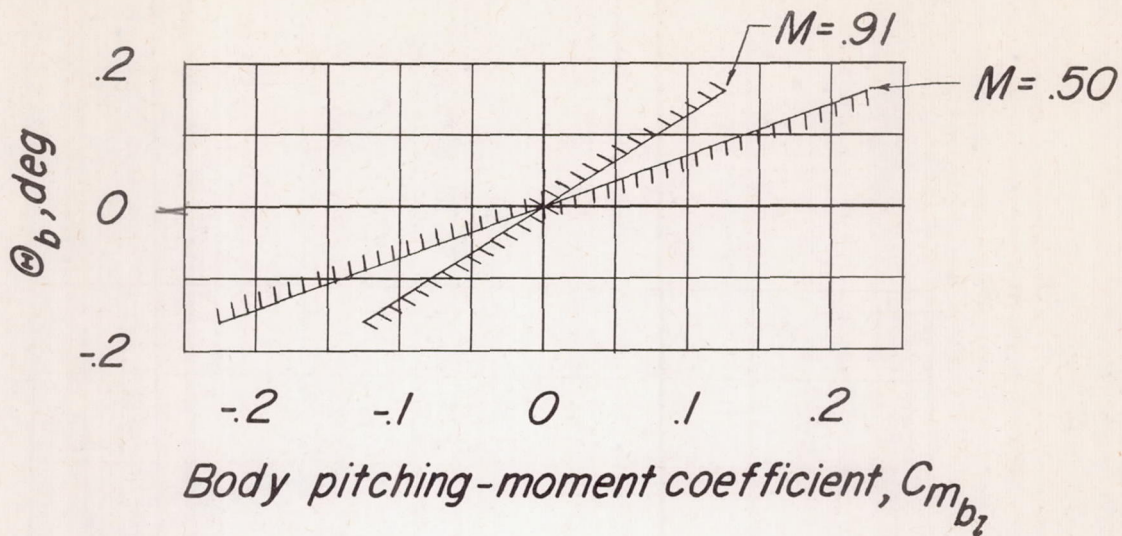


Figure 6.- Deflection characteristics of the body under load.

CONFIDENTIAL

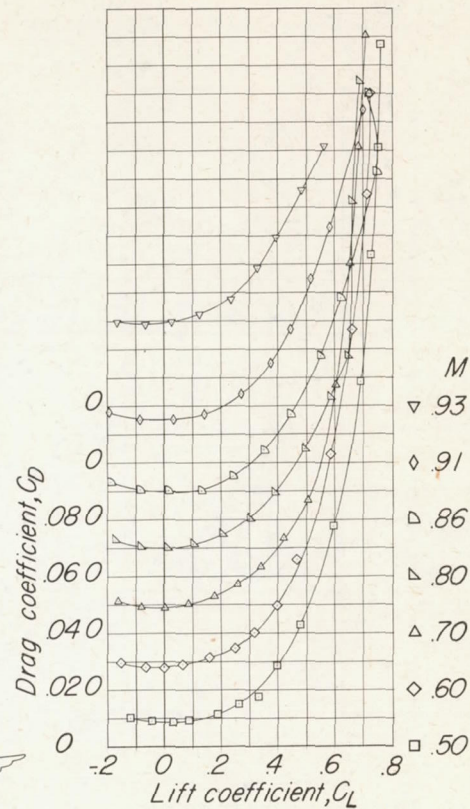
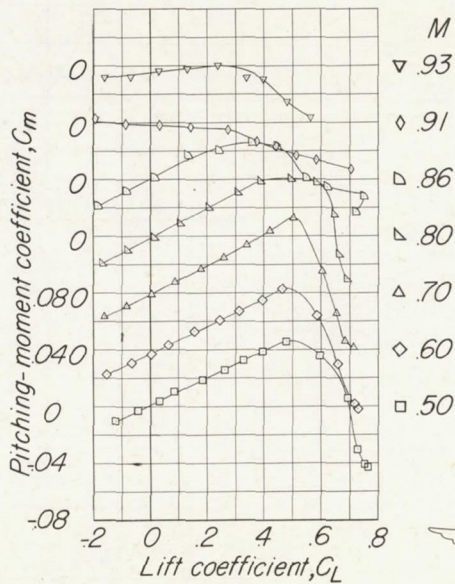
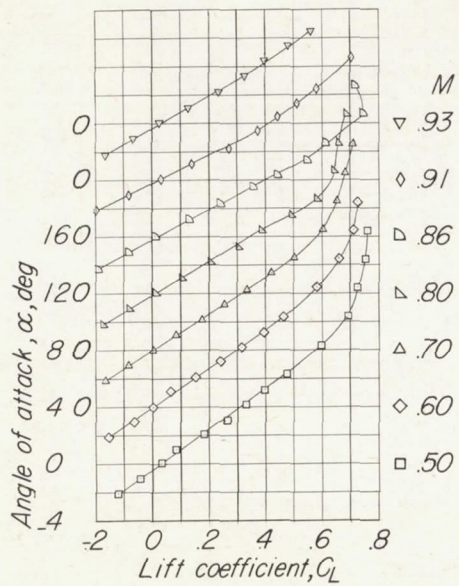
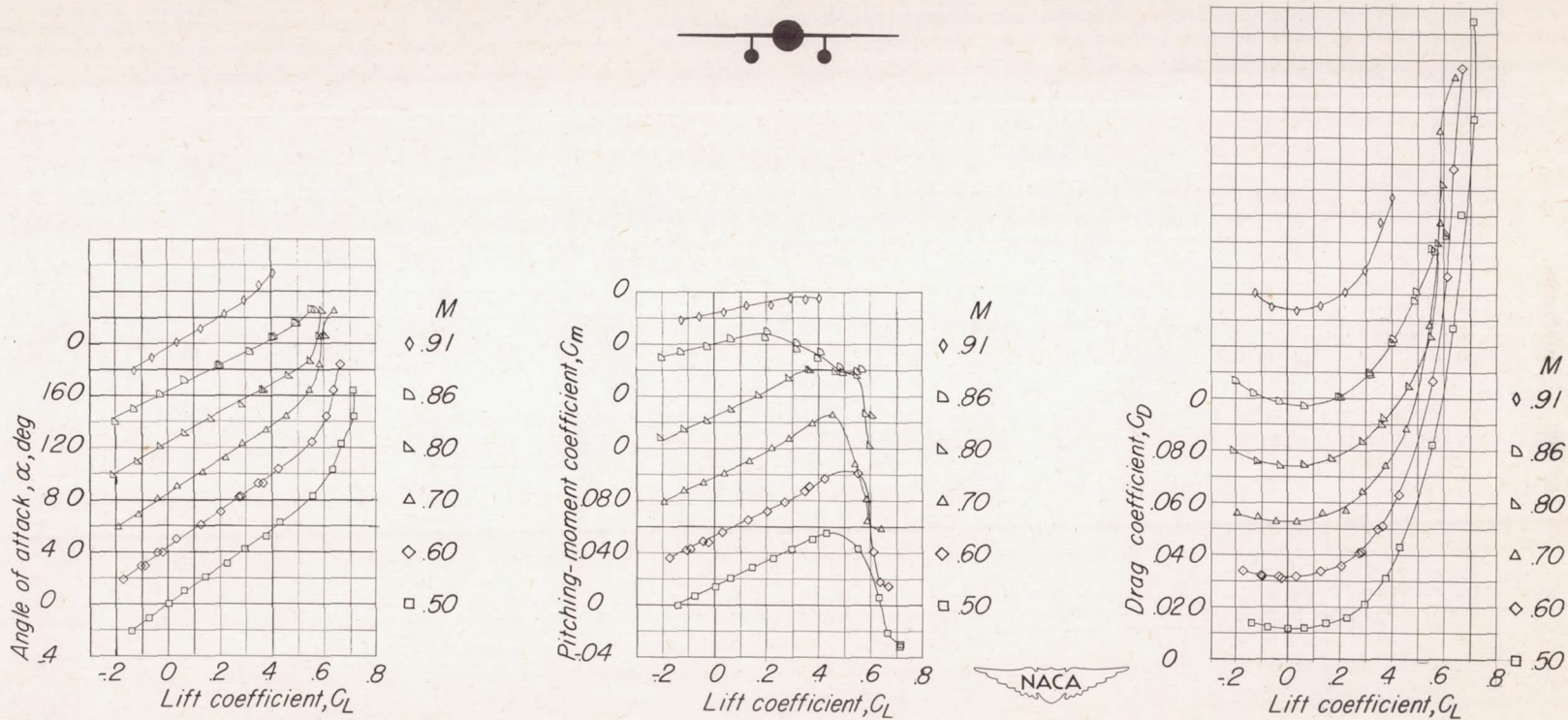


Figure 7.- Aerodynamic characteristics of basic model.

CONFIDENTIAL

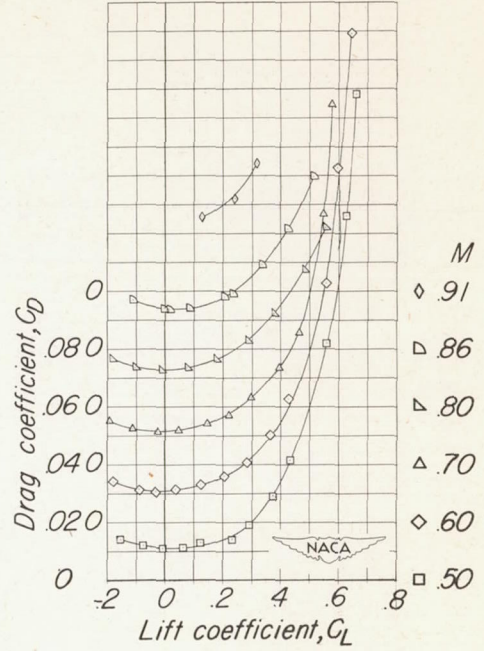
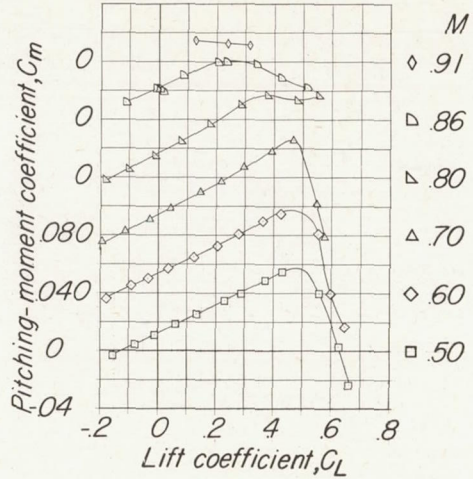
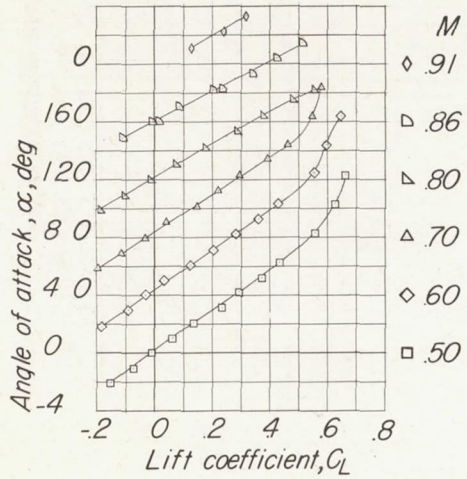


(a) Underwing-inboard bodies, long pylons.

Figure 8.- Aerodynamic characteristics of model with bodies in several locations on wing.



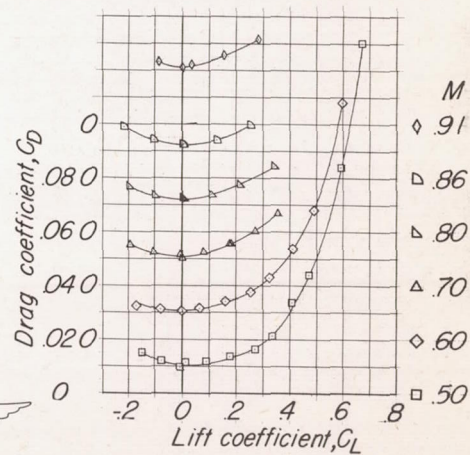
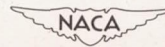
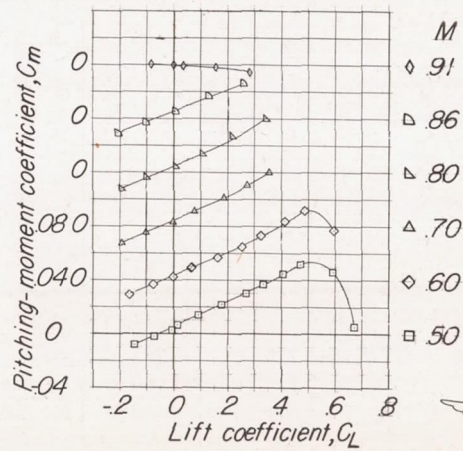
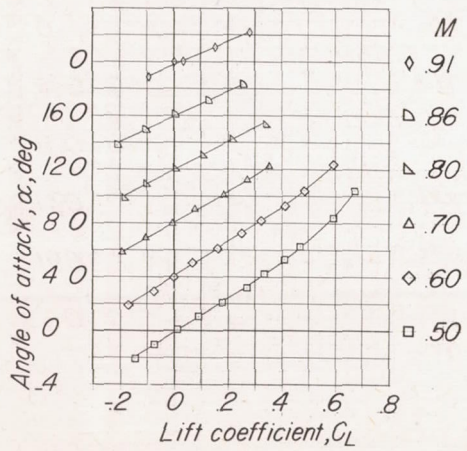
CONFIDENTIAL



(b) Underwing-inboard bodies, short pylons.

Figure 8.- Continued.

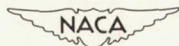
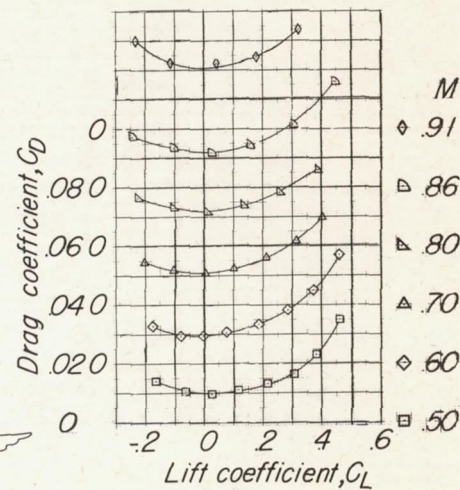
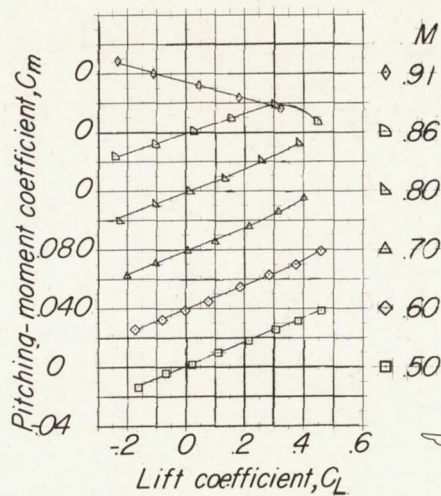
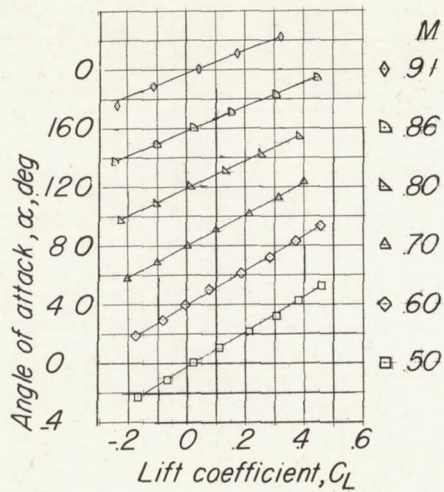
CONFIDENTIAL



(c) Underwing tip bodies.

Figure 8.- Continued.





(d) Tip bodies.

Figure 8.- Concluded.

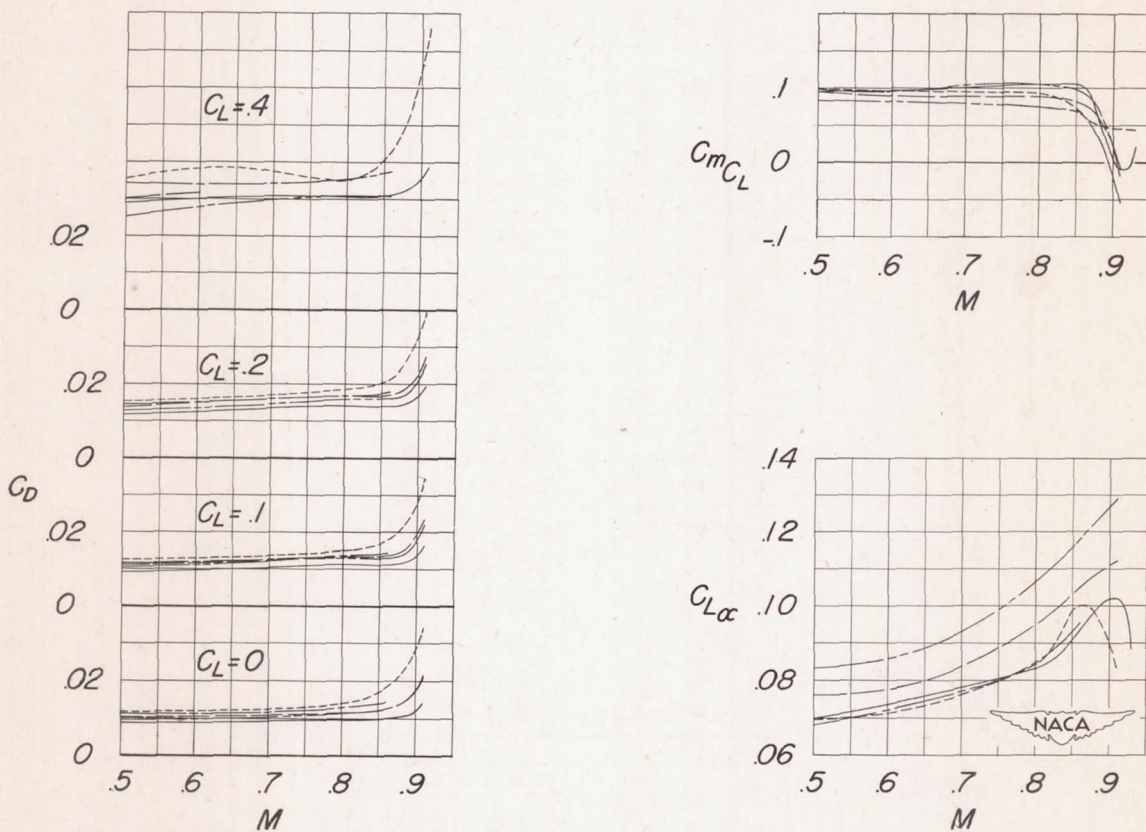
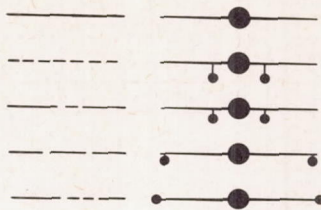


Figure 9.- Summary of effects of bodies in several positions on aerodynamic characteristics of model.

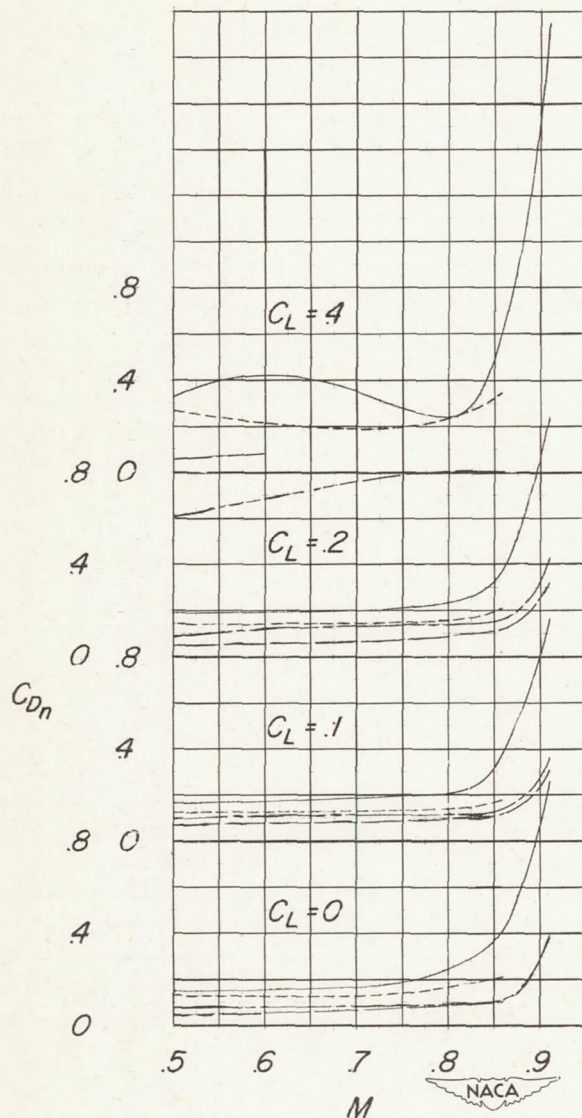
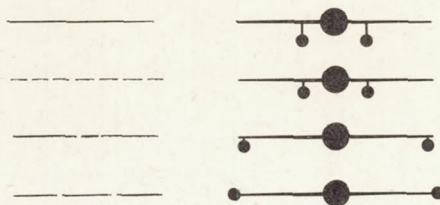
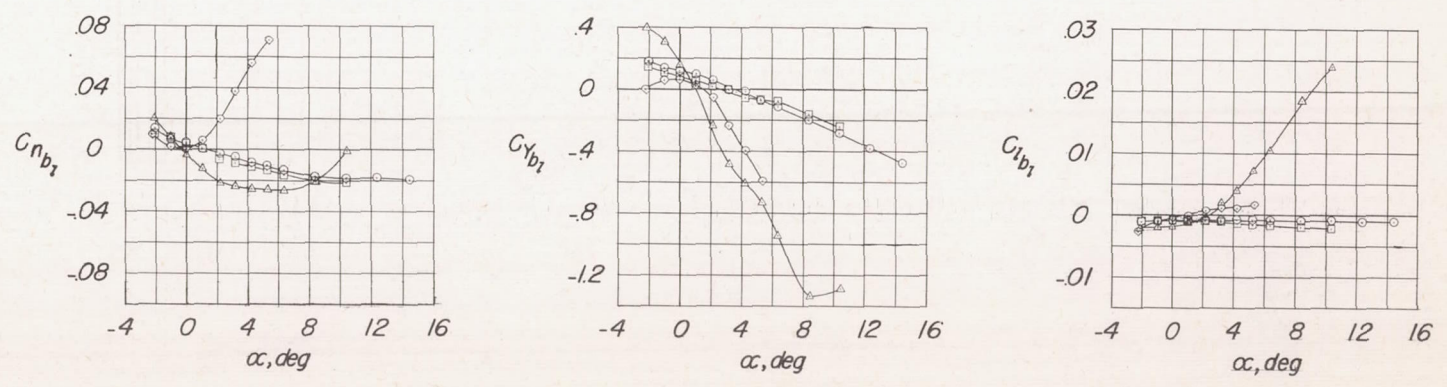
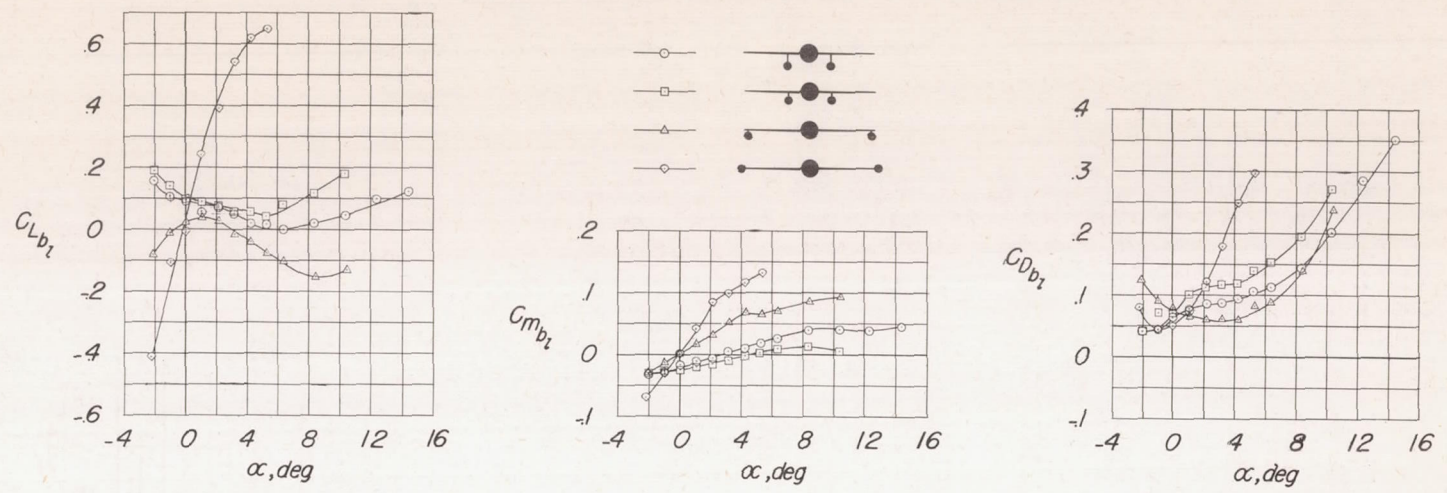
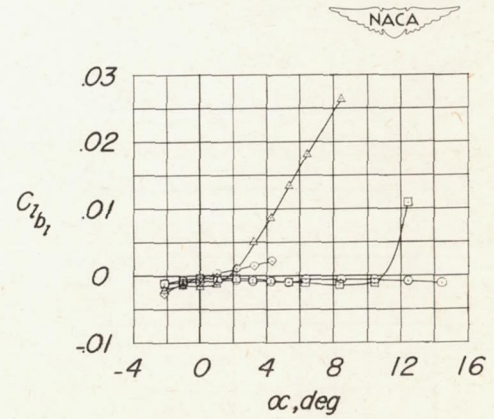
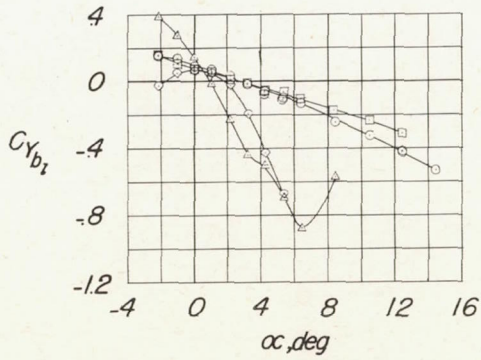
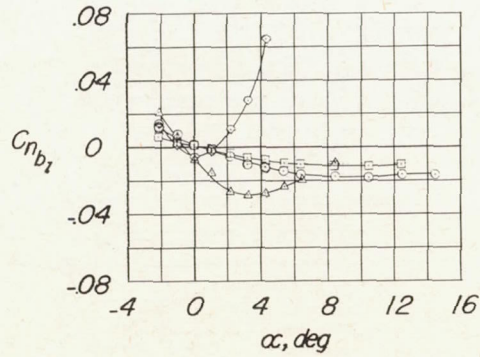
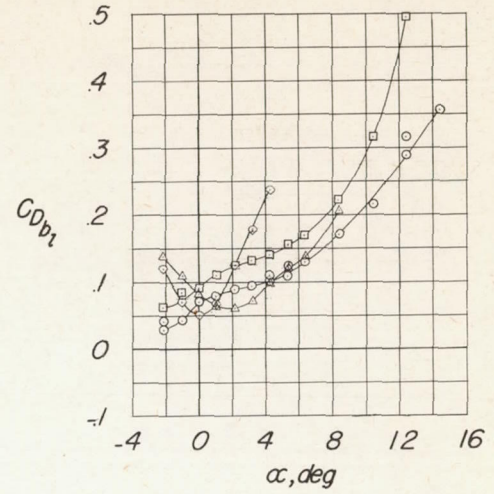
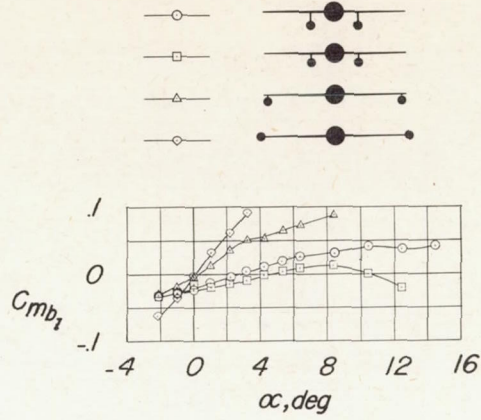
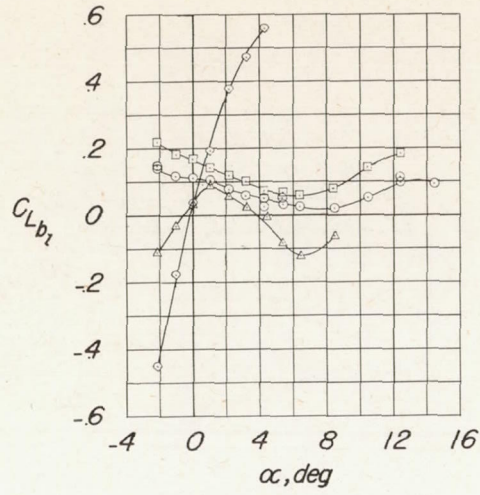


Figure 10.- Installation-drag characteristics of model with body in several positions on wing.



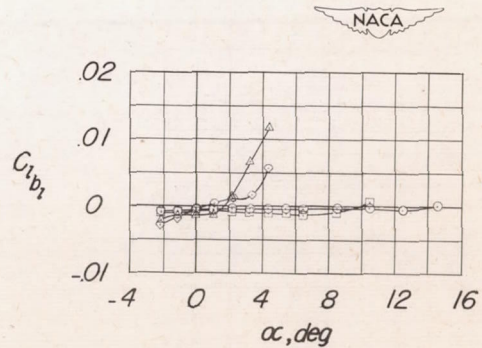
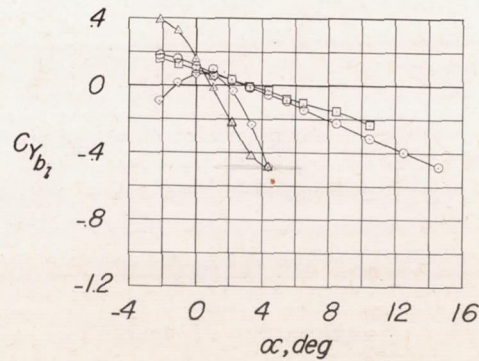
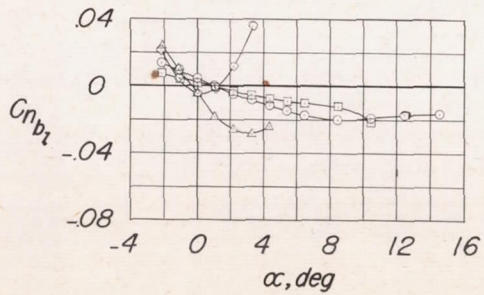
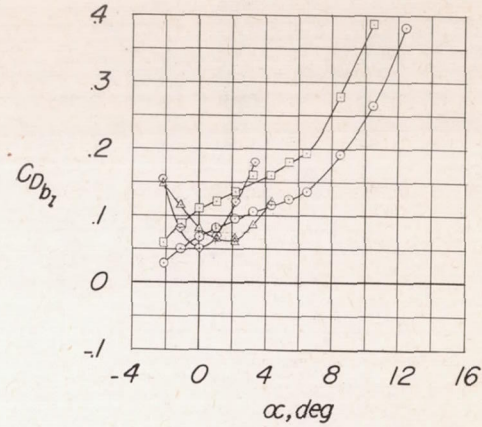
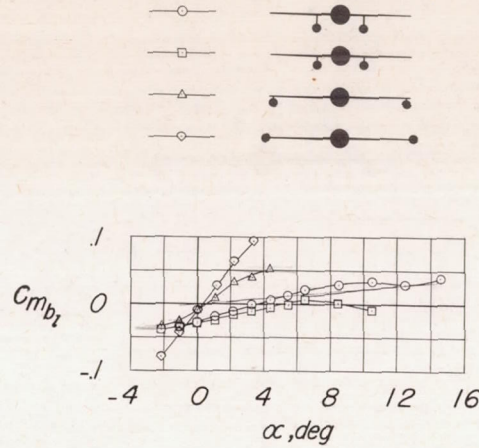
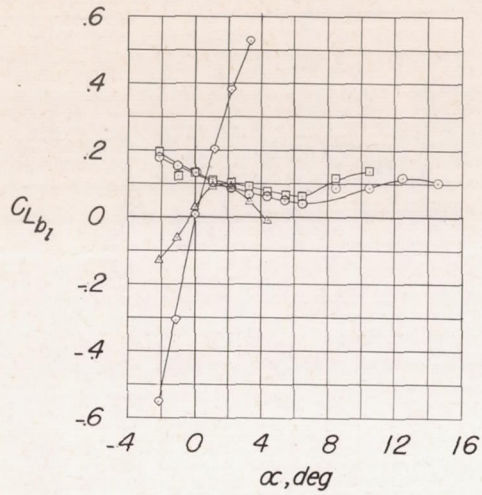
(a) M = 0.50.

Figure 11.- Aerodynamic characteristics of body in several locations on wing of model.



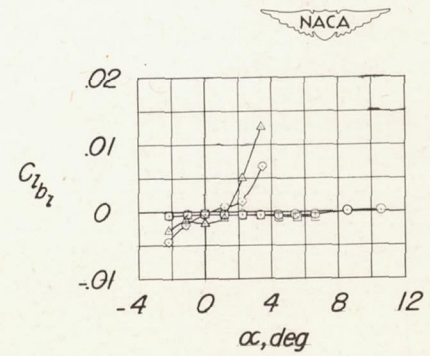
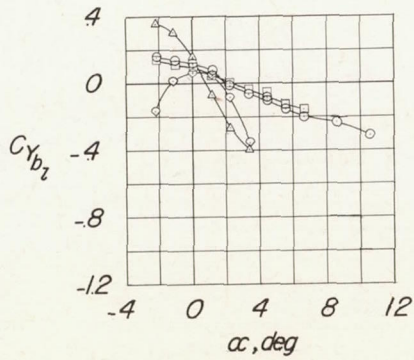
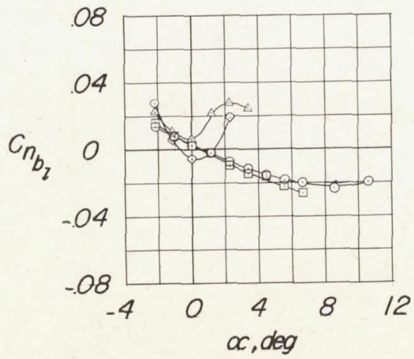
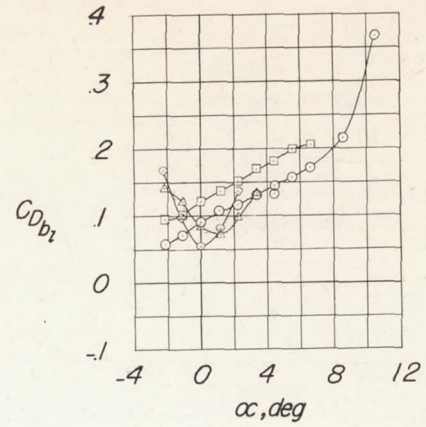
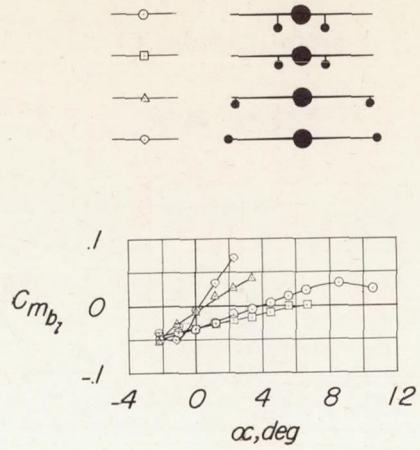
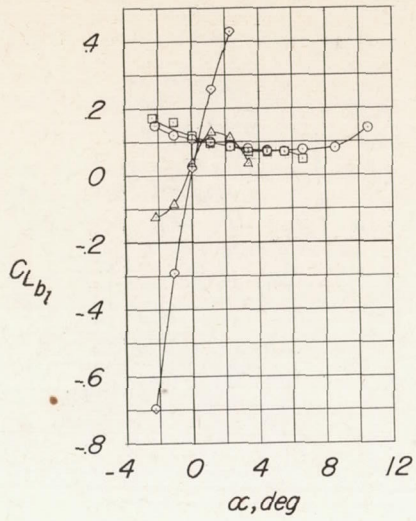
(b) $M = 0.60$.

Figure 11.- Continued.



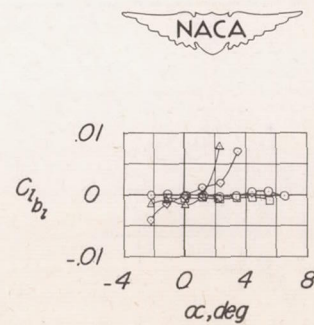
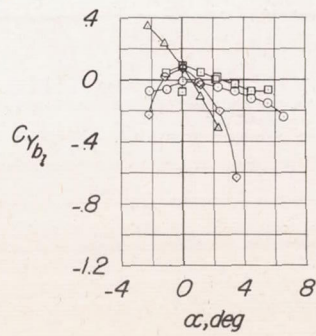
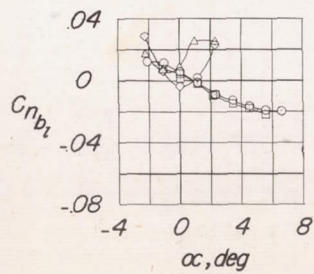
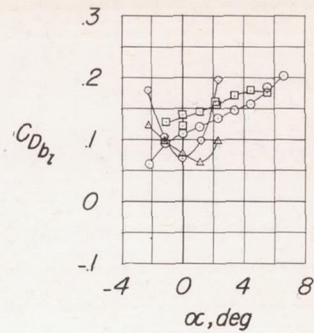
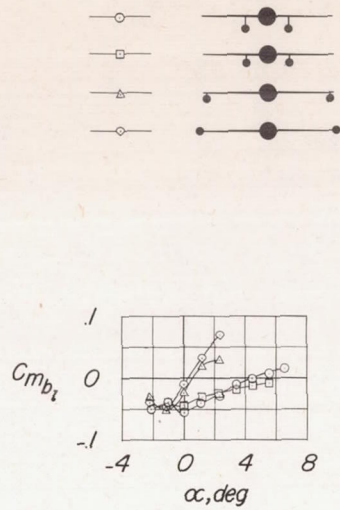
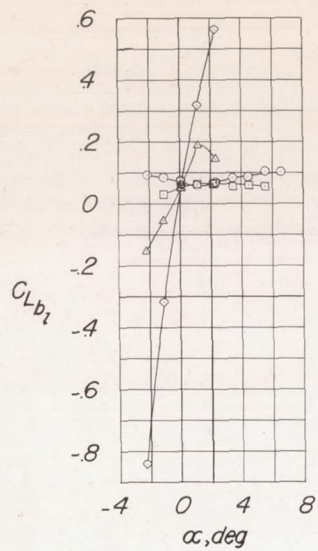
(c) $M = 0.70$.

Figure 11.- Continued.



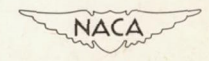
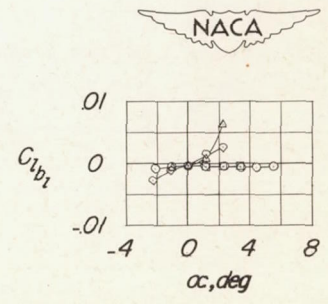
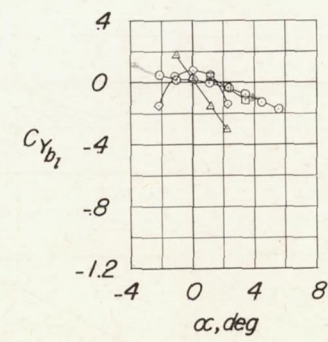
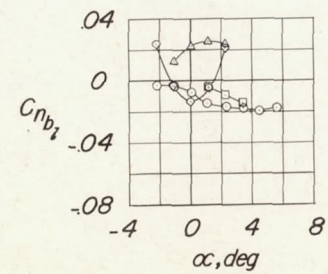
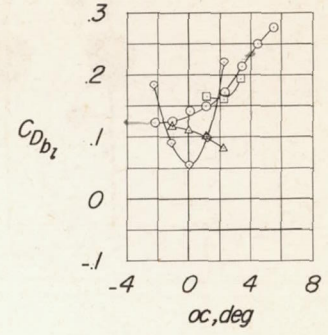
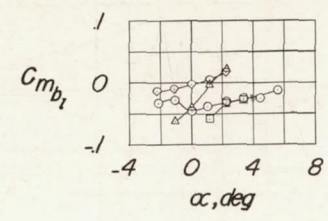
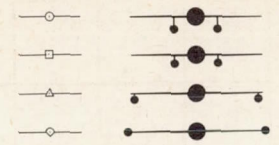
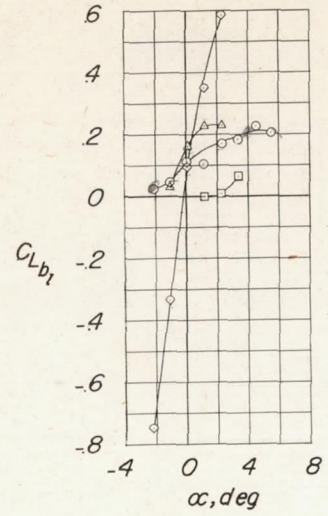
(d) $M = 0.80$.

Figure 11.- Continued.



(e) $M = 0.86$.

Figure 11.- Continued.



(f) M = 0.91.

Figure 11.- Concluded.

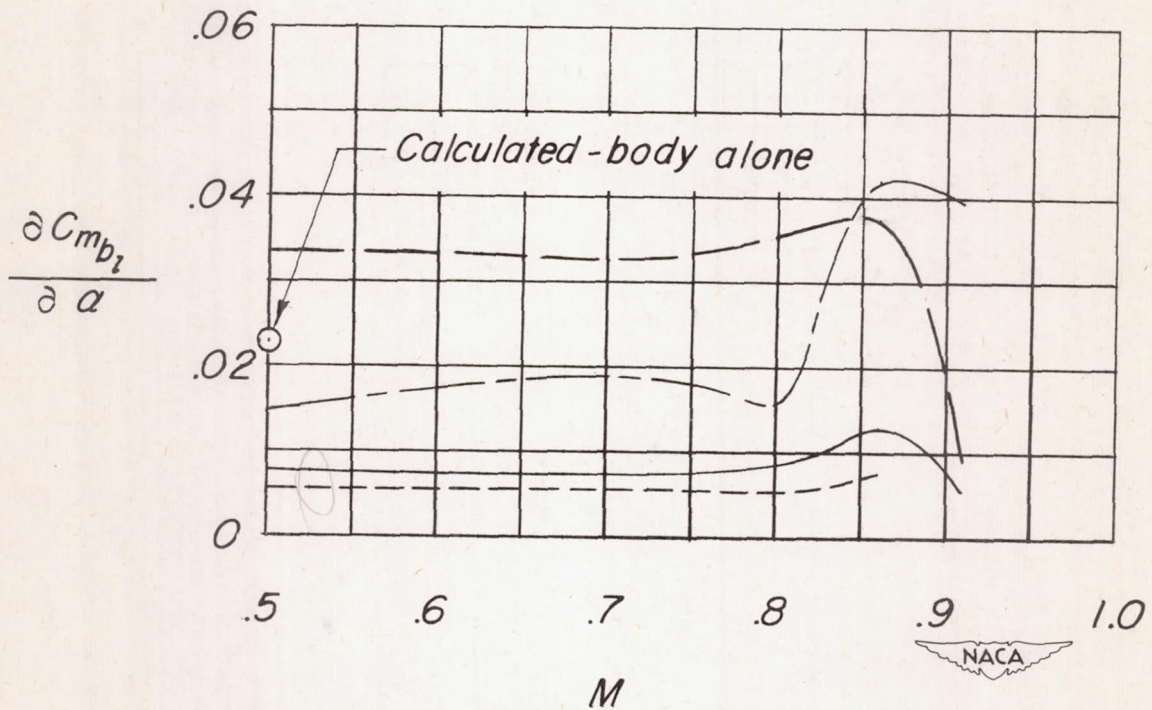
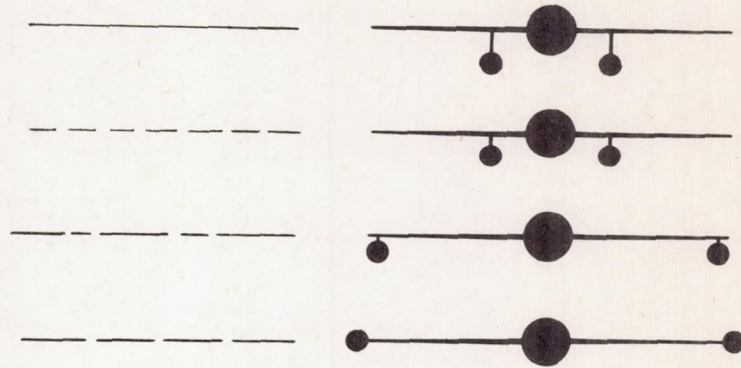
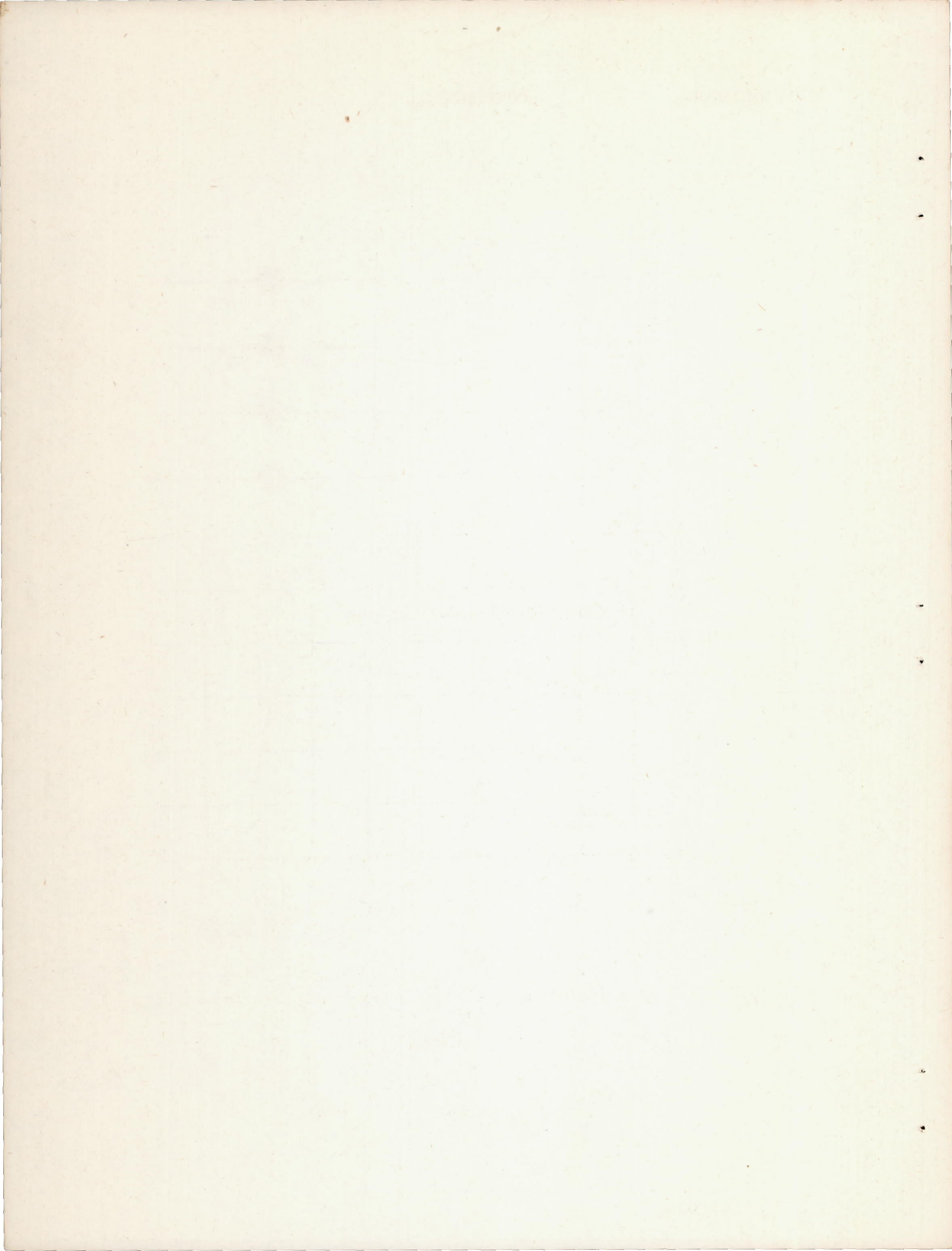
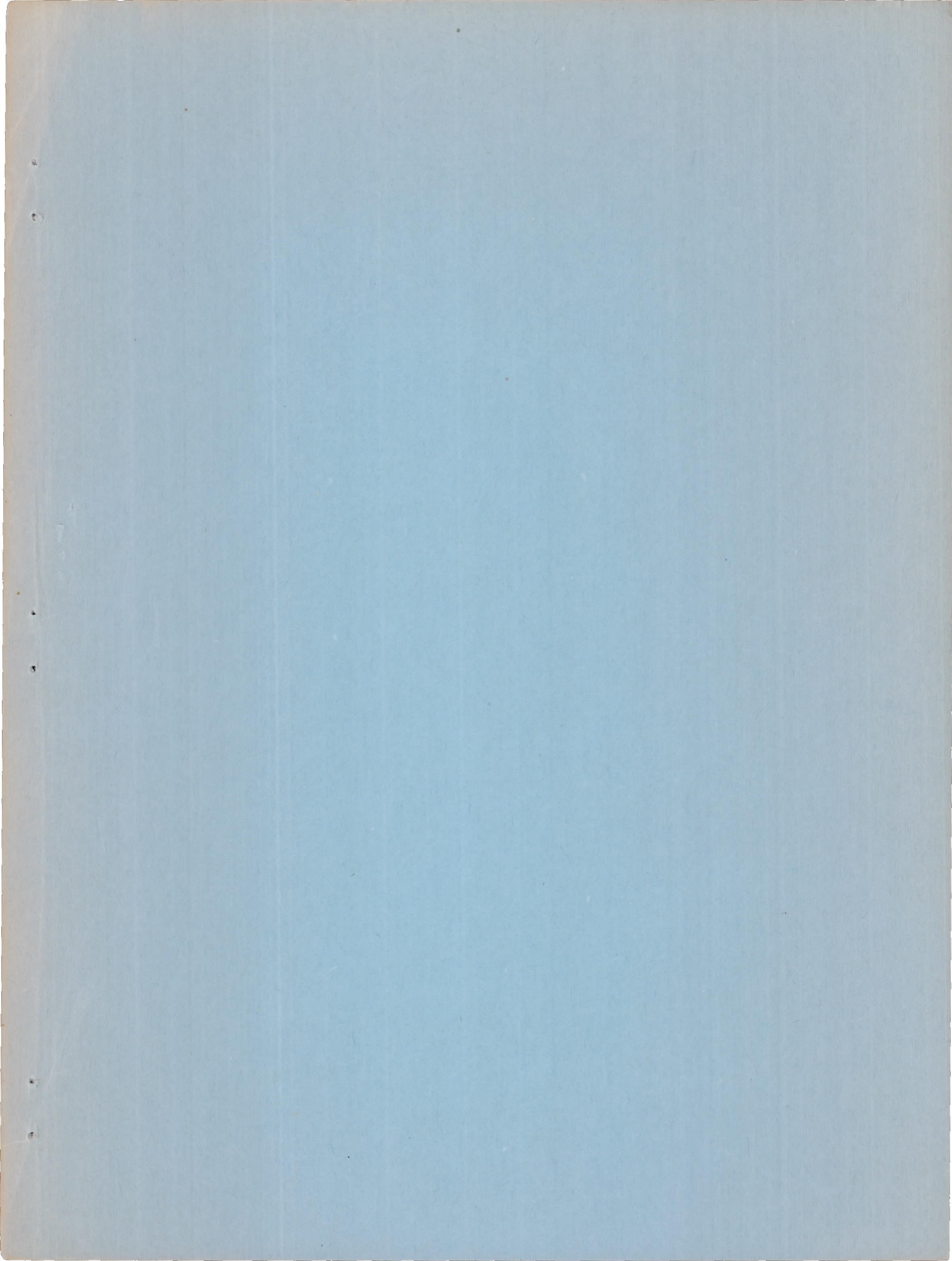


Figure 12.- Pitch characteristics of body in several positions on wing of model.





SECURITY INFORMATION

FEB 21 1974

CONFIDENTIAL

CONFIDENTIAL